FINITE DIFFERENCE METHOD SOLUTION OF MAGNETOHYDRODYNAMIC FLOW IN CHANNELS WITH ELECTRICALLY CONDUCTING AND SLIPPING WALLS

A THESIS SUBMITTED TO
THE GRADUATE SCHOOL OF NATURAL AND APPLIED SCIENCES
OF
MIDDLE EAST TECHNICAL UNIVERSITY

BY

SİNEM ARSLAN

IN PARTIAL FULFILLMENT OF THE REQUIREMENTS
FOR
THE DEGREE OF MASTER OF SCIENCE
IN
MATHEMATICS

MAY 2018

Approval of the thesis:

FINITE DIFFERENCE METHOD SOLUTION OF MAGNETOHYDRODYNAMIC FLOW IN CHANNELS WITH ELECTRICALLY CONDUCTING AND SLIPPING WALLS

submitted by **SİNEM ARSLAN** in partial fulfillment of the requirements for the degree of **Master of Science in Mathematics Department, Middle East Technical University** by,

Prof. Dr. Halil Kalıpçılar _____
Dean, Graduate School of **Natural and Applied Sciences**

Prof. Dr. Yıldıray Ozan _____
Head of Department, **Mathematics**

Prof. Dr. Münevver Tezer _____
Supervisor, **Department of Mathematics, METU**

Examining Committee Members:

Assoc. Prof. Dr. Ayhan Aydın
Department of Mathematics, Atılım University _____

Prof. Dr. Münevver Tezer
Department of Mathematics, METU _____

Assoc. Prof. Dr. Canan Bozkaya
Department of Mathematics, METU _____

Date: _____

I hereby declare that all information in this document has been obtained and presented in accordance with academic rules and ethical conduct. I also declare that, as required by these rules and conduct, I have fully cited and referenced all material and results that are not original to this work.

Name, Last Name: SİNEM ARSLAN

Signature :

ABSTRACT

FINITE DIFFERENCE METHOD SOLUTION OF MAGNETOHYDRODYNAMIC FLOW IN CHANNELS WITH ELECTRICALLY CONDUCTING AND SLIPPING WALLS

ARSLAN, SİNEM
M.S., Department of Mathematics
Supervisor : Prof. Dr. Münevver Tezer

May 2018, 68 pages

In this thesis, the laminar, steady and fully developed magnetohydrodynamic (MHD) flow is considered in a pipe (channel) along with the z-axis under an external magnetic field applied perpendicular to the pipe. The velocity and the induced magnetic field depend only on the plane coordinates x and y on the cross-section of the pipe (duct) when the flow reaches to fully-developed case. This results in two-dimensional MHD duct flow. When the lateral channel walls are extended to infinity the flow is considered between two parallel plates (Hartmann flow). Then, the variations of the velocity and the induced magnetic field are only with respect to the coordinate y between the plates which are perpendicular to the external magnetic field and the problem becomes one-dimensional MHD flow between parallel plates. The finite difference method (FDM) is used to solve the governing equations of 1D and 2D MHD flow problems with the boundary conditions which include both the slip and the varying conductivity of the walls. The numerical results obtained from FDM discretized equations

are compared with the exact solution derived for the 1D MHD flow between parallel plates with the most general case of slipping and variably conducting boundary conditions. On the other hand, for the validation of the numerical results obtained from the FDM for the 2D MHD flow in a square duct with the exact solution, the case of no-slip and insulated duct walls is considered and the agreement is obtained. Also, for both of the 1D and the 2D MHD flow problems, the velocity of the fluid and the induced magnetic field are simulated for each special case of boundary conditions including no-slip to highly slipping and insulated to perfectly conducting plates. The well-known characteristics of the MHD flow and the influences of slipping and electrically conducting plates on the flow and the induced magnetic field are observed. Thus, the FDM which is simple to implement, enables one to depict the effects of Hartmann number, conductivity parameter and the slip parameter on the behavior of both the velocity of the fluid and the induced magnetic field at a small expense.

Keywords: MHD Flow, FDM, Slipping Velocity, Variable Conductivity

ÖZ

ELEKTRİKÇE GEÇİRGEN VE KAYMA SINIR KOŞULLU KANALLARDA MAGNETOHİDRODİNAMİK AKIŞIN SONLU FARK YÖNTEM ÇÖZÜMÜ

ARSLAN, SİNEM
Yüksek Lisans, Matematik Bölümü
Tez Yöneticisi : Prof. Dr. Münevver Tezer

Mayıs 2018 , 68 sayfa

Bu tezde; laminer, kanallardaki zamandan bağımsız ve tam gelişmiş, z-ekseni boyunca uzanan bir boru (kanal) içerisinde olan ve boruya dik olarak uygulanan dış manyetik alan etkisindeki magnetohidrodinamik (MHD) akış ele alınmıştır. Akış tam gelişmiş duruma ulaştığında, hız ve indüklenen manyetik alan, borunun (kanalın) enine kesitinde sadece x ve y düzlem koordinatlarına bağlıdır. Bu, iki-boyutlu MHD kanal akışı ile sonuçlanır. Yanal kanal duvarları sonsuza kadar uzatıldığında, akış iki paralel levha arasında kabul edilir (Hartmann akışı). Daha sonra, hızın ve indüklenen manyetik alanın değişimleri, dış manyetik alana dik olan plakalar arasında sadece y koordinatina bağlı olur ve MHD akış problemi birbirine parallel plakalar arasında bir-boyutlu hale gelir. Duvarlarda hem kayma hem de değişken iletkenliği içeren sınır koşullarına sahip olan bir- ve iki-boyutlu MHD akış problemlerini oluşturan denklemleri çözmek için sonlu fark yöntemi (FDM) kullanılmıştır. Sonlu farkla ayrıklaştırılmış denklemlerden elde edilen yaklaşık sonuçlar, en genel kayma ve değişken iletken sınır koşullarına

sahip olan birbirine paralel plakalar arasındaki bir-boyutlu MHD akışı için elde edilen gerçek çözüm ile karşılaştırılmıştır. Öte yandan, kare bir kanal içerisindeki iki-boyutlu MHD akışı için sonlu fark yönteminden elde edilen yaklaşık çözümlerin gerçek çözümlerle doğrulanması için, kaymayan ve yalıtılmış kanal duvarları durumu göz önünde bulundurulmuş ve çözümlerin birbirleriyle uyuştukları elde edilmiştir. Aynı zamanda, bir- ve iki-boyutlu MHD akış problemlerinin her ikisi için de, kaymayan sınır koşulundan yüksek kayma sınır koşuluna ve yalıtılmıştan tam geçirgen plakalara kadar her bir özel sınır koşulu durumu için akışkan hızının ve indüklenen manyetik alanın simulasyonları yapılmıştır. MHD akışın iyi bilinen özellikleri ile kayma ve elektirikçe geçirgen koşullu plakaların akış ve indüklenen manyetik alan üzerindeki etkileri gözlemlenmiştir. Sonuç olarak, uygulanması kolay olan sonlu fark yöntemi; Hartmann sayısı, geçirgenlik parametresi ve kayma parametresinin hem akışkan hızının hem de indüklenen manyetik alanın üzerindeki etkisini göstermemizi sağlamıştır.

Anahtar Kelimeler: Magnetohidrodinamik Akış, Sonlu Fark Metodu, Kayma Sınır Koşulu, Değişken Geçirgenlik

To my family

ACKNOWLEDGMENTS

I would like to express my immense gratitude to my supervisor Prof. Dr. Münevver Tezer for her continuous support, valuable contributions and patience during the preparation of this thesis. I consider it an honor to work with her and this thesis would not have been possible without her precious guidance and persistent help.

I would also like to thank to my family for their unlimited patience and encouragement through all my life.

TABLE OF CONTENTS

LIST OF TABLES

TABLES

LIST OF FIGURES

FIGURES

NOMENCLATURE

MHD	Magnetohydrodynamics
FDM	Finite Difference Method
1D	one-dimensional
2D	two-dimensional
$\vec{V} = (0, 0, u)$	velocity field
$\vec{B} = (0, B_0, b)$	magnetic field
$\vec{H} = (0, H_0, h)$	magnetic field
$\mu_e \vec{H} = \vec{B}$	magnetic field
$\vec{E}$	electric field
$\vec{f}$	force
$\vec{j}$	electric current density
$\vec{n}$	unit outward normal to the boundary
P	pressure
Ha	Hartmann number
α	slip length
c	conductivity parameter
μ	viscosity
ν	kinematic viscosity
ρ	density
σ	electrical conductivity
μ_e	magnetic permeability
B_0	intensity of the applied magnetic field
U_0	characteristic velocity
L_0	characteristic length
x, y	Cartesian coordinates
h	increment in the x- and y-directions

CHAPTER 1

INTRODUCTION

The boundary value problem, or in short the BVP, is a problem which includes ordinary or partial differential equations with specified conditions on the boundary of the domain in which the problem is defined. To have a well-defined BVP, some conditions of the unknown have to be prescribed on the boundary of the region. Three types of boundary conditions as Dirichlet, Neumann or Robin type boundary condition may be specified when the unknown itself, the normal derivative of the unknown or a linear combination of them are given on the boundary, respectively. Boundary value problems are obtained as consequences of some physical phenomenas in fluid dynamics, magnetohydrodynamics etc. They can be identified with three types of differential equations; elliptic, parabolic or hyperbolic. The problems considered here are of elliptic type.

Fluid dynamics is a branch of applied science that is concerned with the movement of liquids or gases, that is the 'flow of a fluid'. It describes the behavior of the fluid and it is based on two main branches which are fluid mechanics and fluid statics. Magnetohydrodynamics (MHD) is a discipline which is arisen from the main results of fluid mechanics and electrodynamics. It considers the flow of an electrically conducting fluid (water, liquid metals) that are exposed to an external magnetic field and/or an electric current [10]. So, it investigates the influence of these external effects on the behavior of the flow of electrically conducting fluids. Hartmann [6] who studied the MHD flow between parallel planes introduced the study of magnetohydrodynamics and his results provided an insight for understanding the working principles of MHD flow.

MHD has applications in almost every area of our daily life and in engineering

such as magnetic cooling systems, magnetic refrigerators, water treatment devices. Basically, there are several devices whose working principles are based on MHD effects such as MHD pumps, generators, brakes, flow meters and blood flow measurement. Indeed MHD is highly effective in many areas from technology to industry. In technological applications of MHD, its utilizations like being simple and very rugged in operation enables it to be used in technical devices. On the other hand, MHD has many advantages for industrial applications such as nuclear power stations, crystal growth and metallurgical process industry. Magnetohydrodynamics has been so progressed that it is started to be used also in astrophysics which considers planets, stars and galaxies.

In this chapter, some physical laws are introduced leading to MHD equations. As a result of basic principles such as conservation of mass, conservation of momentum and Ampere's law, the combination of Navier-Stokes equations of fluid dynamics including Lorentz force and Maxwell's equations of electromagnetism through Ohm's law form the governing equations of MHD flow. The derivation of the MHD flow equations is given in the most general form in terms of the velocity and pressure of the fluid and the induced magnetic field as problem unknowns. Then, these full MHD equations are simplified for 1D MHD flow between parallel plates and 2D MHD flow in rectangular channels (ducts) which are considered and solved in the next two chapters. Then, the literature survey on the studies related to these problems is given. Finally, the plan of the thesis is expressed.

1.1 MHD Equations

We consider the steady, laminar, fully-developed flow of an incompressible, viscous, electrically conducting fluid. The equations leading to MHD channel flow equations are listed below with corresponding physical laws;

$$\nabla.\vec{V} = 0 \qquad \text{Continuity equation} \tag{1.1}$$

$$\vec{f} - gradP + \mu\nabla^2\vec{V} = \rho(\vec{V}.\nabla)\vec{V} \qquad \text{Navier-Stokes equations} \tag{1.2}$$

$$\vec{f} = \vec{j} \times \vec{B} \qquad \text{Lorentz force} \tag{1.3}$$

$$\vec{j} = \sigma(\vec{E} + \vec{V} \times \vec{B}) \qquad \text{Ohm's law} \tag{1.4}$$

$$\nabla \times \vec{H} = \vec{j} \qquad \text{Ampere's law} \tag{1.5}$$

$$\nabla \times \vec{E} = \vec{0} \qquad \text{Electric field is irrotational} \tag{1.6}$$

$$\nabla.\vec{j} = 0 \qquad \text{Net flux of electric current is zero} \tag{1.7}$$

$$\nabla.\vec{H} = 0 \qquad \text{Magnetic induction is solenoidal} \tag{1.8}$$

with $\vec{j}$, $\vec{H}$, $\vec{E}$, P and $\vec{V}$, and μ, ρ, σ, μ_e are the electric current density, magnetic field, electric field, pressure and the velocity of the fluid, and viscosity, density, electrical conductivity and magnetic permeability of the fluid, respectively. In the absence of electric field $\vec{E}$, Ohm's law reduces to $\vec{j} = \nabla \times \vec{H} = \sigma(\vec{V} \times \vec{B})$. Taking the curl of both sides of Ohm's law (1.4) gives

$$\nabla \times \vec{j} = \sigma\nabla \times (\vec{E} + \vec{V} \times \vec{B})$$

and since $\vec{B} = \mu_e\vec{H}$, it becomes with $\vec{E} = 0$

$$\nabla \times \vec{j} = \sigma\nabla \times \vec{E} + \sigma\mu_e\nabla \times (\vec{V} \times \vec{H}) = \sigma\mu_e\nabla \times (\vec{V} \times \vec{H}).$$

Substituting $\vec{j} = \nabla \times \vec{H}$ by Ampere's law (1.5), we obtain

$$\nabla \times (\nabla \times \vec{H}) = \sigma\mu_e\nabla \times (\vec{V} \times \vec{H}). \tag{1.9}$$

Then, the following two vector identities are going to be used to write the latter equation in a compact form

$$\nabla \times (\nabla \times \vec{H}) = curlcurl\vec{H} = graddiv\vec{H} - \nabla^2\vec{H}$$
$$\nabla \times (\vec{V} \times \vec{H}) = curl(\vec{V} \times \vec{H}) = (\vec{H}.\nabla)\vec{V} - (\vec{V}.\nabla)\vec{H} + \vec{V}div\vec{H} - \vec{H}div\vec{V}.$$

Since $div\vec{H} = 0$ and $div\vec{V} = 0$ from (1.8) and (1.1), respectively, Equation (1.9) becomes the magnetic induction equation

$$\nabla^2\vec{H} + \sigma\mu_e(\vec{H}.\nabla)\vec{V} = 0 \tag{1.10}$$

since $\vec{V}.\nabla = 0$ for a 1D or 2D MHD channel flow with $\vec{V} = (0, 0, u)$ and $\vec{H} = (0, H_0, h)$, $\vec{B} = (0, B_0, b)$ where u and b are the channel axis velocity and the induced magnetic field. Now, let us use the momentum equation (1.2) with the Lorentz force. It can be rewritten by using (1.3) and (1.5) as

$$\mu_e(curl\vec{H} \times \vec{H}) - gradP + \mu\nabla^2\vec{V} = \rho(\vec{V}.\nabla)\vec{V}. \tag{1.11}$$

Differentiating both sides with respect to z gives $grad\left(\dfrac{\partial P}{\partial z}\right) = 0$ since all the other variables are independent of the variable z. This means that $\dfrac{\partial P}{\partial z}$ is a constant. Since $\vec{V}.\nabla = 0$ as mentioned above, the Equation (1.11) becomes

$$\mu_e(curl\vec{H} \times \vec{H}) + \mu\nabla^2\vec{V} = gradP. \tag{1.12}$$

Then, the vector form of the latter equation is

$$\left(-\mu_e h\frac{\partial h}{\partial x}, -\mu_e h\frac{\partial h}{\partial y}, \mu_e H_0\frac{\partial h}{\partial y}\right) + \mu\left(0, 0, \nabla^2 u\right) = \left(\frac{\partial P}{\partial x}, \frac{\partial P}{\partial y}, \frac{\partial P}{\partial z}\right) \tag{1.13}$$

with component wise equality as

$$\begin{aligned} \frac{\partial P}{\partial x} &= -\mu_e h\frac{\partial h}{\partial x} \\ \frac{\partial P}{\partial y} &= -\mu_e h\frac{\partial h}{\partial y} \\ \frac{\partial P}{\partial z} &= \mu_e H_0\frac{\partial h}{\partial y} + \mu\nabla^2 u. \end{aligned} \tag{1.14}$$

On the other hand, the magnetic induction Equation (1.10) in the vector form implies that

$$\nabla^2(0, H_0, h) + \sigma\mu_e\left(0, 0, H_0\frac{\partial u}{\partial y}\right) = 0. \tag{1.15}$$

Finally, the z-components of the momentum Equations (1.14) and the magnetic induction Equations (1.15) are coupled as

$$\begin{aligned} \mu_e H_0\frac{\partial h}{\partial y} + \mu\nabla^2 u &= \frac{\partial P}{\partial z} \\ \nabla^2 h + \sigma\mu_e H_0\frac{\partial u}{\partial y} &= 0 \end{aligned} \tag{1.16}$$

or

$$\begin{aligned} \mu\nabla^2 u + \frac{B_0}{\mu_e}\frac{\partial b}{\partial y} &= \frac{\partial P}{\partial z} \\ \frac{1}{\mu_e}\nabla^2 b + \sigma B_0\frac{\partial u}{\partial y} &= 0 \end{aligned} \tag{1.17}$$

since $\mu_e\vec{H} = \vec{B}$, that is, $\mu_e(0, H_0, h) = (0, B_0, b)$. These coupled MHD channel flow equations are valid for both 1D MHD flow between parallel plates and 2D MHD channel flow in a rectangular channel (duct) when $u = u(y)$, $b = b(y)$ and $u = u(x, y)$, $b = b(x, y)$, respectively.

Now, the nondimensionalization process of the Equations (1.17) are going to be shown by introducing the dimensionless variables as

$$\bar{u} = \frac{u}{U_0}, \quad \bar{b} = \frac{b(\sigma\mu)^{-1/2}}{U_0\mu_e}, \quad \bar{x} = \frac{x}{L_0} \quad \text{and} \quad \bar{y} = \frac{y}{L_0}$$

where $U_0 = -\dfrac{L_0^2}{\mu}\dfrac{\partial P}{\partial z}$ is the characteristic velocity (pipe axis velocity) and L_0 is the characteristic length (half distance between the parallel plates or one side of the rectangular duct). So, we have the new variables

$$u = \bar{u}U_0, \quad b = U_0\mu_e\sqrt{\sigma\mu}\bar{b}, \quad x = \bar{x}L_0, \quad \text{and} \quad y = \bar{y}L_0 \tag{1.18}$$

with the new differential operators

$$\frac{\partial}{\partial x} = \frac{1}{L_0}\frac{\partial}{\partial \bar{x}}, \quad \frac{\partial}{\partial y} = \frac{1}{L_0}\frac{\partial}{\partial \bar{y}}, \quad \frac{\partial^2}{\partial x^2} = \frac{1}{L_0^2}\frac{\partial^2}{\partial \bar{x}^2}, \quad \frac{\partial^2}{\partial y^2} = \frac{1}{L_0^2}\frac{\partial^2}{\partial \bar{y}^2}. \tag{1.19}$$

Substituting the dimensionless variables (1.18) and the operators (1.19) into the Equations in (1.17), we obtain

$$\begin{aligned} \nabla^2\bar{u} + \frac{B_0L_0\sqrt{\sigma}}{\sqrt{\mu}}\frac{\partial \bar{b}}{\partial y} &= -1 \\ \nabla^2\bar{b} + \frac{B_0L_0\sqrt{\sigma}}{\sqrt{\mu}}\frac{\partial \bar{u}}{\partial y} &= 0. \end{aligned} \tag{1.20}$$

Hence, we can substitute u and b instead of $\bar{u}$ and $\bar{b}$ into the Equations (1.20) to get

$$\begin{aligned} \nabla^2 u + Ha\frac{\partial b}{\partial y} &= -1 \\ \nabla^2 b + Ha\frac{\partial u}{\partial y} &= 0 \end{aligned} \tag{1.21}$$

which give the governing dimensionless 1D or 2D coupled MHD channel flow equations. The Hartmann number Ha is defined as $Ha = \dfrac{B_0L_0\sqrt{\sigma}}{\sqrt{\mu}}$, and $\nabla^2 = \dfrac{\partial^2}{\partial x^2} + \dfrac{\partial^2}{\partial y^2}$ is the Laplace operator. When the 1D MHD flow is considered between

parallel plates, the velocity and the induced magnetic field are equations of y only as $\vec{V} = (0, 0, u(y))$, $\vec{B} = (0, B_0, b(y))$ and the Equations (1.21) take the form

$$\begin{aligned} &\frac{d^2u}{dy^2} + Ha\frac{db}{dy} = -1 \\ &\qquad\qquad\qquad\qquad -1 < y < 1. \\ &\frac{d^2b}{dy^2} + Ha\frac{du}{dy} = 0 \end{aligned} \tag{1.22}$$

In the 2D MHD flow, $\vec{V} = (0, 0, u(x, y))$, $\vec{B} = (0, B_0, b(x, y))$ in Equations (1.21) and the domain is the rectangular duct Ω. Thus, the 1D and 2D MHD flow problems given in the Equations (1.22) and (1.21) are going to be solved with the most general boundary conditions (slip and variably conducting walls)

$$u \pm \alpha\frac{du}{dy} = 0 \quad \text{and} \quad \pm\frac{db}{dy} + \frac{1}{c}b = 0 \quad \text{at} \quad y = \pm 1 \tag{1.23}$$

and

$$u \pm \alpha\frac{\partial u}{\partial n} = 0 \quad \text{and} \quad b \pm c\frac{\partial b}{\partial n} = 0 \quad \text{on} \quad \partial\Omega, \tag{1.24}$$

respectively. Here, α is the slip length of the slipping velocity and c is the conductivity parameter.

1.2 Literature Survey

Magnetohydrodynamics started with the investigation of Hartmann and Lazarus [6] who studied the MHD flow between parallel planes and their results provided an insight for understanding the working principles of MHD flow. They studied on the flow of mercury as a conducting fluid in pipes of different cross-sections. Shercliff [12] considered the steady motion of an electrically conducting and viscous fluid in the presence of imposed transverse magnetic field for non-conducting walls. Also, he derived the exact solution of the problem for certain cases and gave a theoretical view on the study of Hartmann layers for square duct and circular pipe. Gold [5] obtained an exact solution for no-slip and non-conducting walls in a circular pipe. Hunt and Stewartson [8] studied laminar flow of an electrically conducting liquid in a rectangular duct under a uniform transverse magnetic field. They discussed the effect of the conductivity of the walls

like perfectly conducting walls parallel to the magnetic field and non-conducting walls perpendicular to the field. Similarly, Temperley and Todd [17] studied also the effects of wall conductivity on the solution of MHD duct flow by using classical theory, but at high Hartmann numbers. Singh and Lal [13] used the finite difference method (FDM) with Kantorovich and Crank-Nicolson methods (for unsteady problems) to solve the MHD axial flow in a triangular pipe under transverse magnetic field for small values of Hartmann number. They also used the finite element method (FEM) in different cross-sections of a pipe such as rectangular, triangular and circular in order to solve the MHD channel flow problem numerically for Hartmann numbers $\leqslant 5$, [14]. Then, Tezer-Sezgin and Köksal [20] used FEM for the steady MHD flow through a rectangular pipe with arbitrarily conducting walls for several values of Hartmann number between 5 and 100. In addition, Chutia and Deka [3] solved steady, 2-dimensional MHD flow through a square duct under the action of transverse magnetic field with insulated walls by using finite difference method at high Hartmann numbers up to 500.

Later on, in the 1980's, the boundary element method (BEM) is included to the basic domain discretization methods such as FDM and FEM for solving the MHD duct flow problems which discretizes only the boundary of the problem domain. The resulting system of equations are quite small in size compared to FEM and FDM discretized system of equations sizes. Both BEM and dual reciprocity boundary element method (DRBEM) have been used for solving MHD duct flow problems in different geometries with several boundary conditions. Tezer-Sezgin [18] used BEM with constant elements for solving MHD duct flow with moderate Hartmann numbers and similarly Carabineanu et al. [2] utilized the BEM for solving MHD problem in a conducting medium. Besides, Liu and Zhu [9] considered the MHD duct flow with arbitrary wall conductivity in the presence of a transverse external magnetic field with various inclined angles by using DRBEM.

The MHD flow problems are also investigated with the hydrodynamic slip condition at the interface between the electrically conducting fluid and the insulating wall. There are several studies on the MHD flow problems with slipping con-

dition. Smolentsev [15] gave the analytical solutions of the Hartmann flow and fully-developed flow in a rectangular duct with slip condition and also analyzed the thickness of the Hartmann and the side walls under the effect of slip condition. Rivero and Cuevas [11] used one and two-dimensional MHD flow models with different slipping walls and gave the analytical and numerical calculations, and also analyzed the effect of the slip length on the flow rate.

Bozkaya and Tezer-Sezgin [1] used BEM application after they derived the fundamental solution for the coupled convection–diffusion type equations and they solved the MHD duct flow problems with the most general form of wall conductivities and for values of Hartmann number up to 300 [19]. Hosseinzadeh et al. [7] considered the constant and the continuous linear boundary elements methods (BEMs) to obtain the numerical solution of the coupled equations of MHD flow. They presented a new technique for a general boundary condition (arbitrary wall conductivity) at Hartmann numbers $\leqslant 10^5$. Tao and Ni [16] obtained two analytical solutions by solving the governing equations in the liquid and in the walls coupled with the boundary conditions at fluid-wall interface for MHD flow at a rectangular duct with unsymmetrical walls of arbitrary conductivity.

In this thesis, the numerical solution of the 1D and the 2D MHD flow equations in a long pipe of rectangular cross-section have been investigated by using the finite difference method. The problem solutions are sought when both the slip and the conductivity boundary conditions are effective on each Hartmann and side walls, which are not available in the literature yet by using the FDM. The numerical solutions are obtained by using a suitable code in Matlab after the discretization of the domain. Also, the exact solution of 1D MHD flow is derived for the most general form of slip and variable conducting end conditions, and the comparison of the exact solution with the numerical solutions show very well agreement even at high Hartmann number values. A similar procedure is used to solve the 2D MHD flow equations with FDM again for the slip and/or variably conducting Hartmann and side walls. The influences of the slipping and the conductivity parameters on the velocity and the induced magnetic field are illustrated with equivelocity and the current lines for increasing values of Hartmann number.

1.3 Plan of the Thesis

In Chapter 1, first of all the fundamental equations of fluid dynamics and electromechanics are introduced. Then, the equations which describe the MHD flow in one-dimensional and two-dimensional cross-sections of the channels are derived by using some vector identities. The non-dimensional forms of the governing equations are obtained with some dimensionless parameters. A general literature survey on the MHD channel flow is given. In the next two chapters the MHD channel flow problems are considered with different types of boundary conditions as four cases according to the slip and/or variably conducting channel walls. These cases are listed in the following table. The last Case 5 is considered only in the 2D MHD flow.

Table 1.1: Cases of wall conditions, α = slip length, c = conductivity parameter.

Case 1.	No-slip and insulated walls ($\alpha = 0$, $c = 0$)
Case 2.	No-slip but variably conducting walls ($\alpha = 0$, c varies)
Case 3.	Slipping but insulated walls (α varies, $c = 0$)
Case 4.	Both slipping and variably conducting walls (α, c varies)
Case 5.	No-slip walls, Hartmann walls are perfectly conducting and side walls are insulated

In Chapter 2, the 1D MHD flow equations are given with the most general type of boundary conditions which involve both the slip and the conductivity parameters. Firstly, the exact solution of the problem is obtained when both the slip and the conductivity parameter exist on the boundary by using variation of parameters technique. Using FDM approximations for the derivatives, a numerical scheme is obtained. Then, inserting the boundary conditions into the discretized equations for each case, a system of linear equations is deduced and then is solved with Gaussian elimination in Matlab. Then, the numerical solutions at discretized points are simulated for varying values of Hartmann number, and slip and conductivity parameters for each case.

In Chapter 3, we consider the 2D MHD channel flow problem for the cases explained in the above Table 1.1. Again, FDM is used for solving the governing equations. Then, the 2D MHD channel flow problem with the most general boundary conditions as in Case 4 is solved by using a general scheme which covers all the cases listed in the Table 1.1. The governing equations of the 2D MHD channel flow problem for the boundary conditions of Case 1 are decoupled since it becomes easier to solve the decoupled equations with this case of boundary conditions. Indeed, the general scheme also gives the solution of the 2D MHD flow problem of Case 1, and the numerical results obtained from both of the coupled and decoupled equations coincide. With the FDM discretization of the domain, both the coupled and decoupled schemes result in linear systems of equations, that is, matrix-vector systems are obtained for the unknown velocity and the induced magnetic field. Then, the linear systems are solved with a suitable code in Matlab to get the solution at discretized points for each case by choosing the values of the slipping and the conductivity parameters. Finally, numerical results and their discussions are presented by explaining the effects of the variable conducting and the slipping boundaries on the solution of the MHD flow for several values of Hartmann number.

In Chapter 4, the summary of what is done in this thesis study and the general findings are expressed.

CHAPTER 2

1D MHD FLOW BETWEEN PARALLEL PLATES

In this chapter, the MHD flow is considered in a long pipe of rectangular cross-section along with the z-axis under the influence of an external magnetic field which is perpendicular to the pipe. Therefore the relevant variables, the velocity u and the induced magnetic field b depend only on the plane coordinates x and y when the flow reaches to fully-developed case. The flow can be considered between two parallel plates when the sides of the pipe parallel to the applied magnetic field are assumed to be extended to $\pm$ infinity (Hartmann flow). Thus, the external magnetic field is perpendicular to the channel walls and the lateral channel walls are at infinity. Now, the variations of the velocity u and the induced magnetic field b are only in one coordinate variable y, and the MHD flow problem becomes 1-dimensional between parallel plates.

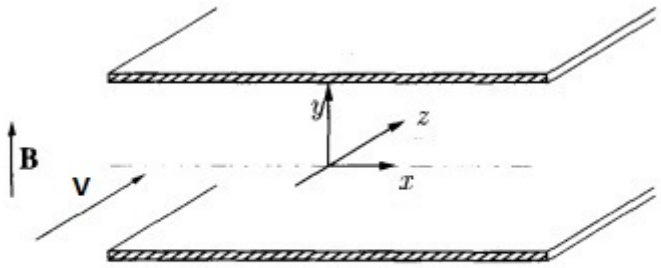

Figure 2.1: Hartmann flow configuration

The finite difference method (FDM) is used to solve the governing 1D MHD equations numerically. The numerical results obtained from the FDM discretized equations have been compared with the exact solution of the problem which is

given in [10] when the plates have no-slip condition for the velocity of the fluid. An accuracy of order 10^{-3} has been observed for both u and b when they are compared with the exact solution even for a large Hartmann number. Further, different type of boundary conditions such as slip velocity condition and insulated and/or conducting end points (plates) are used and in this thesis, the exact solutions are also derived for all of these cases. Thus, we were able to compare our FDM solutions with the exact solutions for the most general cases of the boundary conditions. As a result, the FDM have made us to be able to understand the effect of these type of boundary conditions on the behavior of both the velocity u and the induced magnetic field b at a small computational expense. The volumetric flow rates are also computed for all the cases of boundary conditions considered.

2.1 Formulation of the Problem

The fully developed MHD flow between two parallel plates is reduced to one-dimensional MHD flow when the lateral walls are assumed to be extending to infinity. According to the geometrical configuration in Figure 2.1, both the velocity and the induced magnetic field are in the z-direction but vary only in the y-direction which is the distance between the plates. The governing equations in non-dimensional form for this Hartmann flow are the coupled convection-diffusion equations

$$\begin{aligned} &\frac{d^2u}{dy^2} + Ha\frac{db}{dy} = -1 \\ &\qquad\qquad\qquad\qquad \text{in} \quad -1 < y < 1 \\ &\frac{d^2b}{dy^2} + Ha\frac{du}{dy} = 0 \end{aligned} \tag{2.1}$$

where $u(y)$ and $b(y)$ are the velocity and the induced magnetic field, respectively. Ha is the Hartmann number and c is the conductivity parameter. Hartmann number is given as $Ha = L_0 B_0 \sqrt{\frac{\sigma}{\rho\nu}}$ where L_0 is the characteristic length, B_0 is the intensity of the external magnetic field, σ, ρ and ν are the electrical conductivity, the density and the kinematic viscosity of the fluid, respectively. The boundary conditions for the velocity and the induced magnetic field are taken in

the most general form as Robin's type which contain the slipping velocity and the variable conductivity as

$$u \pm \alpha \frac{du}{dy} = 0, \qquad \pm \frac{db}{dy} + \frac{1}{c} b = 0 \qquad \text{at} \quad y = \pm 1. \tag{2.2}$$

Here $c \to 0$ corresponds to electrically insulating walls (plates) and $c \to \infty$ to electrically perfectly conducting walls, and α is the slip length of the slipping velocity at the end points. Also, $\alpha = 0$ implies the no-slip boundary conditions (non-slipping plates).

2.2 Exact Solution

The exact solution of the problem (2.1) for the case of no-slip boundary conditions ($\alpha = 0$), that is, $u = 0$ at $y = \pm 1$ is given in [3, 11] as

$$\begin{aligned} u(y) &= \hat{u} \left[1 - \frac{\cosh((Ha)y)}{\cosh(y)} \right], \\ b(y) &= -\frac{y}{Ha} + \hat{u} \frac{\sinh((Ha)y)}{\cosh((Ha)y)}, \end{aligned} \tag{2.3}$$

with the characteristic magnitude of the velocity

$$\hat{u} = \frac{1}{Ha} \frac{c+1}{cHa + \tanh(Ha)}. \tag{2.4}$$

Next, we will consider the cases of slip but insulated walls and also slipping and conducting walls. The exact solutions for these cases are derived below. Firstly, the new variables U_1 and U_2 are defined by

$$U_1(y) = u + b \qquad \text{and} \qquad U_2(y) = u - b$$

in order to make the Equations in (2.1) decoupled. Adding and subtracting them gives

$$\frac{d^2 U_1}{dy^2} + Ha \frac{dU_1}{dy} = -1 \tag{2.5}$$

$$\frac{d^2 U_2}{dy^2} - Ha \frac{dU_2}{dy} = -1. \tag{2.6}$$

Now, the method of variation of parameters is going to be used to obtain the unknowns U_1 and U_2 and then going back to the original variables $u = \dfrac{U_1 + U_2}{2}$

and $b = \dfrac{U_1 - U_2}{2}$, the exact solution of the problem (2.1) with the boundary conditions (2.2) is going to be obtained.

From the homogeneous part of the Equation (2.5), we have the characteristic equation

$$r^2 + (Ha)r = 0.$$

So,

$$U_1^h(y) = a + f\exp(-(Ha)y)$$

for some nonzero constants a and f. Thus, $y_1 = a$ and $y_2 = \exp(-(Ha)y)$ are the fundamental set of solutions and the Wronskian of them is $W(y_1, y_2) = -a(Ha)\exp(-(Ha)y)$. Then, the particular solution $U_1^p(y)$ is obtained by variation of parameters formula as

$$U_1^p(y) = -a\int \frac{\exp(-(Ha)y)(-1)}{-a(Ha)\exp(-(Ha)y)}dy + \exp(-(Ha)y)\int \frac{a(-1)}{-a(Ha)\exp(-(Ha)y)}dy$$

$$U_1^p(y) = \frac{-y}{Ha} + \frac{1}{(Ha)^2}$$

Hence,

$$U_1(y) = U_1^h + U_1^p = g + f\exp(-(Ha)y) - \frac{y}{Ha}$$

where $g = a + \dfrac{1}{(Ha)^2}$. Similarly, the homogeneous part of the equation (2.6) gives

$$U_2^h(y) = l + d\exp((Ha)y)$$

for some nonzero constants l and d. Then, the particular solution is of the form

$$U_2^p(y) = \frac{y}{Ha} - \frac{1}{(Ha)^2}.$$

Thus, the general solution is given by

$$U_2(y) = U_2^h + U_2^p = k + d\exp((Ha)y) + \frac{y}{Ha}$$

where $k = l - \dfrac{1}{(Ha)^2}$ and f and d are constants to be determined. Finally, going back to the original variables, we have

$$u(y) = m + \frac{1}{2}\left(f\exp(-(Ha)y) + d\exp((Ha)y)\right)$$

$$b(y) = l + \frac{1}{2}\left(f\exp(-(Ha)y) - d\exp((Ha)y)\right) - \frac{y}{Ha}$$

where $m = \dfrac{g+k}{2}$ and $l = \dfrac{g-k}{2}$. Using the boundary conditions in the Equation (2.2), it can be easily observed that the solutions are of the following form

$$u(y) = -\frac{f+d}{2}\left(\alpha(Ha)\sinh(Ha) + \cosh(Ha)\right) + \frac{1}{2}\left(f\exp(-(Ha)y) + d\exp((Ha)y)\right)$$
$$b(y) = -\frac{f-d}{2}\left(\cosh(Ha) + c(Ha)\sinh(Ha)\right) + \frac{1}{2}\left(f\exp((-Ha)y) - d\exp((Ha)y)\right) - \frac{y}{Ha}.$$

For simplicity, we can assume $f = d = A$ by fixing to the same constant A. Thus, we get

$$u(y) = -A\left(\alpha(Ha)\sinh(Ha) + \cosh(Ha)\right) + A\cosh((Ha)y)$$
$$b(y) = -A\sinh((Ha)y) - \frac{y}{Ha}.$$

Now, this form of the solutions satisfy the boundary condition for u in the Equation (2.2) automatically and from the variable conductivity condition for b the fixed constant A is obtained. Let us define $A = \tilde{u}$. Thus, the exact solution of the problem (2.1) with the general boundary conditions (2.2) is obtained as

$$u(y) = -\tilde{u}(\alpha(Ha)\sinh(Ha) + \cosh(Ha)) + \tilde{u}\cosh((Ha)y) \tag{2.7}$$
$$b(y) = -\tilde{u}\sinh((Ha)y) - \frac{y}{Ha} \tag{2.8}$$

where

$$\tilde{u} = -\frac{1}{Ha}\frac{c+1}{c(Ha)\cosh(Ha) + \sinh(Ha)}. \tag{2.9}$$

This exact solution given by (2.7)-(2.9) for the slip velocity and variable conductivity conditions on the plates is reduced to the exact solution given in [10] for the no-slip and insulated wall conditions when $\alpha = 0$ and $c = 0$ are taken.

2.3 FDM Solution of 1D MHD Flow Equations with Different types of Boundary Conditions

- **Case 1.**

For this case, we choose the slip length $\alpha = 0$ and the conductivity parameter $c = 0$ at the boundary points $y = \pm 1$. So, the problem becomes

$$\begin{aligned} &\frac{d^2u}{dy^2} + Ha\frac{db}{dy} = -1 \\ &\qquad\qquad\qquad\qquad \text{in} \quad -1 < y < 1 \\ &\frac{d^2b}{dy^2} + Ha\frac{du}{dy} = 0 \end{aligned}$$

with the no-slip and insulated end conditions

$$u = 0, \qquad b = 0 \qquad \text{at} \quad y = \pm 1. \tag{2.10}$$

The exact solution is given in Equations (2.3)-(2.4) for $c = 0$. Using central finite difference for the first and the second order derivatives of u and b, we get

$$\begin{aligned} &\frac{u_{j+1} - 2u_j + u_{j-1}}{h^2} + Ha\frac{b_{j+1} - b_{j-1}}{2h} = -1 \\ &\qquad\qquad\qquad\qquad\qquad\qquad\qquad\qquad j = 2, \ldots, N \\ &\frac{b_{j+1} - 2b_j + b_{j-1}}{h^2} + Ha\frac{u_{j+1} - u_{j-1}}{2h} = 0 \end{aligned}$$

where $h = \frac{1-(-1)}{N} = \frac{2}{N}$ is the step size and N is the number of subintervals. Multiplying both sides of the above equations by h^2 gives

$$\begin{aligned} &u_{j+1} - 2u_j + u_{j-1} + \frac{Ha}{2}h\left(b_{j+1} - b_{j-1}\right) = -h^2 \\ &\qquad\qquad\qquad\qquad\qquad\qquad\qquad\qquad j = 2, \ldots, N \\ &b_{j+1} - 2b_j + b_{j-1} + \frac{Ha}{2}h\left(u_{j+1} - u_{j-1}\right) = 0. \end{aligned}$$

From the boundary conditions, we have

$$u_1 = u_{N+1} = 0 \qquad \text{and} \qquad b_1 = b_{N+1} = 0.$$

Thus, we have $2N - 2$ unknowns $u_2, b_2, u_3, b_3, \ldots, u_N, b_N$ in $2N - 2$ equations. Then, we write these equations in matrix-vector system $Ax = z$. Here, the

coefficient matrix A with the size $(2N-2)\times(2N-2)$ contains the step size h and Ha in its entries as shown bellow

$$A=\begin{bmatrix}
-2 & 0 & 1 & \frac{hHa}{2} & 0 & 0 & 0 & 0 & \cdots & 0\\
0 & -2 & \frac{hHa}{2} & 1 & 0 & 0 & 0 & 0 & \cdots & 0\\
1 & -\frac{hHa}{2} & -2 & 0 & 1 & \frac{hHa}{2} & 0 & 0 & \cdots & 0\\
-\frac{hHa}{2} & 1 & 0 & -2 & \frac{hHa}{2} & 1 & 0 & 0 & \cdots & 0\\
\vdots & \vdots & \vdots & \vdots & \vdots & \vdots & \vdots & \vdots & \vdots & \vdots\\
\vdots & \vdots & \vdots & \vdots & \vdots & \vdots & \vdots & \vdots & \vdots & \vdots\\
0 & \vdots & \vdots & \vdots & \vdots & \vdots & \vdots & \vdots & \vdots & 0\\
0 & 0 & \cdots & 0 & 1 & -\frac{hHa}{2} & -2 & 0 & 1 & \frac{hHa}{2}\\
0 & 0 & \cdots & 0 & -\frac{hHa}{2} & 1 & 0 & -2 & \frac{hHa}{2} & 1\\
0 & 0 & \cdots & 0 & 0 & 0 & 1 & -\frac{hHa}{2} & -2 & 0\\
0 & 0 & \cdots & 0 & 0 & 0 & -\frac{hHa}{2} & 1 & 0 & -2
\end{bmatrix}.$$

Also, the unknown vector x includes the velocity and the induced magnetic field components

$$x=\begin{bmatrix}u_2 & b_2 & u_3 & b_3 & \cdots & u_N & b_N\end{bmatrix}^{\mathsf{T}},$$

and the known vector z is of size $2N-2$ given as

$$z=\begin{bmatrix}-h^2 & 0 & -h^2 & 0 & \cdots & -h^2 & 0\end{bmatrix}^{\mathsf{T}}.$$

Then, we deduce the solution $x=A^{-1}z$ by using Gaussian elimination from Matlab which does not compute the inverse directly. The profiles of the velocity and the induced magnetic field are drawn comparing with the exact solution.

- **Case 2.**

For this case, we choose no-slip and variably conducting end points at $y = \pm 1$. So, the problem becomes

$$\begin{aligned} &\frac{d^2u}{dy^2} + Ha\frac{db}{dy} = -1 \\ &\qquad\qquad\qquad\qquad \text{in} \quad -1 < y < 1 \\ &\frac{d^2b}{dy^2} + Ha\frac{du}{dy} = 0 \end{aligned}$$

and

$$u = 0, \qquad \pm\frac{db}{dy} + \frac{1}{c}b = 0 \qquad \text{at} \quad y = \pm 1. \tag{2.11}$$

The exact solution is given by Equations (2.3)-(2.4) for varying values of c.

From the boundary conditions for u, we have

$$u_1 = u_{N+1} = 0.$$

But, b_1 and b_{N+1} are not known explicitly. For the boundary conditions for b, we use forward finite difference at the point $y = -1$ and backward finite difference at the point $y = 1$ for finding b_1 and b_{N+1} in terms of b_2 and b_N, respectively.

- At $y = -1$:

$$-\left(\frac{b_2 - b_1}{h}\right) + \frac{1}{c}b_1 = 0 \quad \Rightarrow \quad b_1 = \frac{c}{c+h}b_2.$$

- At $y = 1$:

$$\left(\frac{b_{N+1} - b_N}{h}\right) + \frac{1}{c}b_{N+1} = 0 \quad \Rightarrow \quad b_{N+1} = \frac{c}{c+h}b_N.$$

Thus, we have again $2N-2$ unknowns $u_2, b_2, u_3, b_3, \ldots, u_N, b_N$ in $2N-2$ equations. Then, we write these equations in a matrix-vector system $Ax = z$. Here, the coefficient matrix A with the size $(2N-2) \times (2N-2)$ differs from the coefficient matrix of Case 1 only in the first two and the last two rows as

$$A = \begin{bmatrix}
-2 & -\frac{(Ha)ch}{2(c+h)} & 1 & \frac{hHa}{2} & 0 & 0 & 0 & 0 & \cdots & 0 \\
0 & \frac{c}{c+h} - 2 & \frac{hHa}{2} & 1 & 0 & 0 & 0 & 0 & \cdots & 0 \\
1 & -\frac{hHa}{2} & -2 & 0 & 1 & \frac{hHa}{2} & 0 & 0 & \cdots & 0 \\
-\frac{hHa}{2} & 1 & 0 & -2 & \frac{hHa}{2} & 1 & 0 & 0 & \cdots & 0 \\
\vdots & \vdots & \vdots & \vdots & \vdots & \vdots & \vdots & \vdots & \vdots & \vdots \\
\vdots & \vdots & \vdots & \vdots & \vdots & \vdots & \vdots & \vdots & \vdots & \vdots \\
0 & \vdots & \vdots & \vdots & \vdots & \vdots & \vdots & \vdots & \vdots & 0 \\
0 & 0 & \cdots & 0 & 1 & -\frac{hHa}{2} & -2 & 0 & 1 & \frac{hHa}{2} \\
0 & 0 & \cdots & 0 & -\frac{hHa}{2} & 1 & 0 & -2 & \frac{hHa}{2} & 1 \\
0 & 0 & \cdots & 0 & 0 & 0 & 1 & -\frac{hHa}{2} & -2 & -\frac{(Ha)ch}{2(c+h)} \\
0 & 0 & \cdots & 0 & 0 & 0 & -\frac{hHa}{2} & 1 & 0 & \frac{c}{c+h} - 2
\end{bmatrix}.$$

The unknown vector x of size $2N-2$ includes the velocity and the induced magnetic field components

$$x = \begin{bmatrix} u_2 & b_2 & u_3 & b_3 & \cdots & u_N & b_N \end{bmatrix}^{\mathsf{T}},$$

and the vector z is of size $2N-2$ given as

$$z = \begin{bmatrix} -h^2 & 0 & -h^2 & 0 & \cdots & -h^2 & 0 \end{bmatrix}^{\mathsf{T}}.$$

Then, we obtain the solution $x = A^{-1}z$ and the profiles of the velocity and the induced magnetic field are drawn for several values of conductivity parameter c. They are compared with the exact solution behaviors given in [10] and obtained by us in Equations (2.3)-(2.4).

- **Case 3.**

For this case, we assume the velocity slip at the insulated boundary points $y = \pm 1$. So, the problem becomes

$$\frac{d^2u}{dy^2} + Ha\frac{db}{dy} = -1$$

$$\text{in} \quad -1 < y < 1$$

$$\frac{d^2b}{dy^2} + Ha\frac{du}{dy} = 0$$

and with the slip condition (α is the slip length)

$$\pm \frac{du}{dy}\alpha + u = 0, \qquad b = 0 \qquad \text{at} \quad y = \pm 1. \tag{2.12}$$

From the boundary conditions for b (insulated end points), we have

$$b_1 = b_{N+1} = 0.$$

But u_1 and u_{N+1} are not known explicitly. For obtaining the boundary conditions for u, we use forward finite difference at the point $y = -1$ and the backward finite difference at the point $y = 1$ and find u_1 and u_{N+1} in terms of u_2 and u_N, respectively.

- At $y = -1$:

$$-\left(\frac{u_2 - u_1}{h}\right)\alpha + u_1 = 0 \quad \Rightarrow \quad u_1 = \frac{\alpha}{\alpha + h}u_2.$$

- At $y = 1$:

$$\left(\frac{u_{N+1} - u_N}{h}\right)\alpha + u_{N+1} = 0 \quad \Rightarrow \quad u_{N+1} = \frac{\alpha}{\alpha + h}u_N.$$

Thus, we have $2N - 2$ unknowns $u_2, b_2, u_3, b_3, \ldots, u_N, b_N$ in $2N - 2$ equations similar to the previous cases. The coefficient matrix A of the system $Ax = z$ is altered in its first two and last two rows corresponding to the slip and insulated end points as

$$A = \begin{bmatrix}
\frac{\alpha}{\alpha+h}-2 & 0 & 1 & \frac{hHa}{2} & 0 & 0 & 0 & 0 & \cdots & 0 \\
-\frac{(Ha)\alpha h}{2(\alpha+h)} & -2 & \frac{hHa}{2} & 1 & 0 & 0 & 0 & 0 & \cdots & 0 \\
1 & -\frac{hHa}{2} & -2 & 0 & 1 & \frac{hHa}{2} & 0 & 0 & \cdots & 0 \\
-\frac{hHa}{2} & 1 & 0 & -2 & \frac{hHa}{2} & 1 & 0 & 0 & \cdots & 0 \\
\vdots & \vdots & \vdots & \vdots & \vdots & \vdots & \vdots & \vdots & \vdots & \vdots \\
\vdots & \vdots & \vdots & \vdots & \vdots & \vdots & \vdots & \vdots & \vdots & \vdots \\
0 & \vdots & \vdots & \vdots & \vdots & \vdots & \vdots & \vdots & \vdots & 0 \\
0 & 0 & \cdots & 0 & 1 & -\frac{hHa}{2} & -2 & 0 & 1 & \frac{hHa}{2} \\
0 & 0 & \cdots & 0 & -\frac{hHa}{2} & 1 & 0 & -2 & \frac{hHa}{2} & 1 \\
0 & 0 & \cdots & 0 & 0 & 0 & 1 & -\frac{hHa}{2} & \frac{\alpha}{\alpha+h}-2 & 0 \\
0 & 0 & \cdots & 0 & 0 & 0 & -\frac{hHa}{2} & 1 & -\frac{(Ha)\alpha h}{2(\alpha+h)} & -2
\end{bmatrix}.$$

The $2N-2$ sized unknown vector x includes the same velocity and the induced magnetic field entries as in the previous cases since u_1 and u_{N+1} are expressed in terms of u_2 and u_N

$$x = \begin{bmatrix} u_2 & b_2 & u_3 & b_3 & \cdots & u_N & b_N \end{bmatrix}^{\mathsf{T}},$$

and the known vector z is of size $2N-2$ given as before

$$z = \begin{bmatrix} -h^2 & 0 & -h^2 & 0 & \cdots & -h^2 & 0 \end{bmatrix}^{\mathsf{T}}.$$

Then, we deduce the solution $x = A^{-1}z$ and the profiles of the velocity and the induced magnetic field are obtained. The FDM solution is in very well agreement with the exact solution (2.7)-(2.9) for $c = 0$ (insulated walls). For increasing values of α one needs to take more points in the discretization of the interval $[-1, 1]$. The slip velocity behavior is shown and discussed in the u-profiles for increasing values of α.

- **Case 4.**

Finally, we choose both the slip condition $\pm\dfrac{du}{dy}\alpha + u = 0$ and the varying conductivity condition $\pm\dfrac{db}{dy} + \dfrac{1}{c}b = 0$ at the boundary points $y = \pm 1$. So, the problem becomes

$$\begin{aligned} &\frac{d^2u}{dy^2} + Ha\frac{db}{dy} = -1 \\ &\qquad\qquad\qquad\qquad \text{in} \quad -1 < y < 1 \\ &\frac{d^2b}{dy^2} + Ha\frac{du}{dy} = 0 \end{aligned}$$

and

$$\pm\frac{du}{dy}\alpha + u = 0, \qquad \pm\frac{db}{dy} + \frac{1}{c}b = 0 \qquad \text{at} \quad y = \pm 1 \tag{2.13}$$

with α the slip length and c the conductivity parameter.

From the boundary conditions for u and b, we use forward finite difference for both $\dfrac{\partial b}{\partial y}$ and $\dfrac{\partial u}{\partial y}$ at the point $y = -1$ and the backward finite difference at the point $y = 1$ in (2.13) to find u_1, u_{N+1} and b_1, b_{N+1}, respectively.

- At $y = -1$:

$$-\left(\frac{u_2 - u_1}{h}\right)\alpha + u_1 = 0 \quad \Rightarrow \quad u_1 = \frac{\alpha}{\alpha + h}u_2.$$

$$-\left(\frac{b_2 - b_1}{h}\right) + \frac{1}{c}b_1 = 0 \quad \Rightarrow \quad b_1 = \frac{c}{c + h}b_2.$$

- At $y = 1$:

$$\left(\frac{u_{N+1} - u_N}{h}\right)\alpha + u_{N+1} = 0 \quad \Rightarrow \quad u_{N+1} = \frac{\alpha}{\alpha + h}u_N.$$

$$\left(\frac{b_{N+1} - b_N}{h}\right) + \frac{1}{c}b_{N+1} = 0 \quad \Rightarrow \quad b_{N+1} = \frac{c}{c + h}b_N.$$

The same $2N - 2$ sized matrix-vector system is obtained with the unknowns $u_2, b_2, u_3, b_3, \ldots, u_N, b_N$. Now, the coefficient matrix with its altered rows according to the boundary conditions becomes

$$A = \begin{bmatrix}
\frac{\alpha}{\alpha+h}-2 & -\frac{(Ha)ch}{2(c+h)} & 1 & \frac{hHa}{2} & 0 & 0 & 0 & 0 & \cdots & 0 \\
-\frac{(Ha)\alpha h}{2(\alpha+h)} & \frac{c}{c+h}-2 & \frac{hHa}{2} & 1 & 0 & 0 & 0 & 0 & \cdots & 0 \\
1 & -\frac{hHa}{2} & -2 & 0 & 1 & \frac{hHa}{2} & 0 & 0 & \cdots & 0 \\
-\frac{hHa}{2} & 1 & 0 & -2 & \frac{hHa}{2} & 1 & 0 & 0 & \cdots & 0 \\
\vdots & \vdots & \vdots & \vdots & \vdots & \vdots & \vdots & \vdots & \vdots & \vdots \\
\vdots & \vdots & \vdots & \vdots & \vdots & \vdots & \vdots & \vdots & \vdots & \vdots \\
0 & \vdots & \vdots & \vdots & \vdots & \vdots & \vdots & \vdots & \vdots & 0 \\
0 & 0 & \cdots & 0 & 1 & -\frac{hHa}{2} & -2 & 0 & 1 & \frac{hHa}{2} \\
0 & 0 & \cdots & 0 & -\frac{hHa}{2} & 1 & 0 & -2 & \frac{hHa}{2} & 1 \\
0 & 0 & \cdots & 0 & 0 & 0 & 1 & -\frac{hHa}{2} & \frac{\alpha}{\alpha+h}-2 & \frac{(Ha)ch}{2(c+h)} \\
0 & 0 & \cdots & 0 & 0 & 0 & -\frac{hHa}{2} & 1 & \frac{(Ha)\alpha h}{2(\alpha+h)} & \frac{c}{c+h}-2
\end{bmatrix}.$$

Again, the unknown vector x which includes the velocity and the induced magnetic field components is of $2N-2$ size as

$$x = \begin{bmatrix} u_2 & b_2 & u_3 & b_3 & \cdots & u_N & b_N \end{bmatrix}^{\mathsf{T}},$$

and the known vector z is also of size $2N-2$ given as

$$z = \begin{bmatrix} -h^2 & 0 & -h^2 & 0 & \cdots & -h^2 & 0 \end{bmatrix}^{\mathsf{T}}.$$

The solution $x = A^{-1}z$ is obtained without forming the inverse of A and the profiles of the velocity and the induced magnetic field are drawn. The results can be compared with the derived exact solution given in Equations (2.7) and (2.9).

2.4 Numerical Results and Discussion

So far, we have obtained the numerical values of the velocity u and the induced magnetic field b by using FDM. For validating these numerical results with the corresponding exact values, we use the so-called *mesh validation* (Figure 2.2) for $Ha = 100$ when the boundary conditions are taken as no-slip velocity and insulated walls (Case 1). Here, N is the number of subintervals in the interval $-1 \leqslant y \leqslant 1$ and it is easily seen that when $N \geqslant 128$ the numerical and exact values are getting close to each other, and they coincide when N increases in which the well agreement is reached for $N \geqslant 256$. Thus, we have observed that the larger N gives numerical result with very good accuracy.

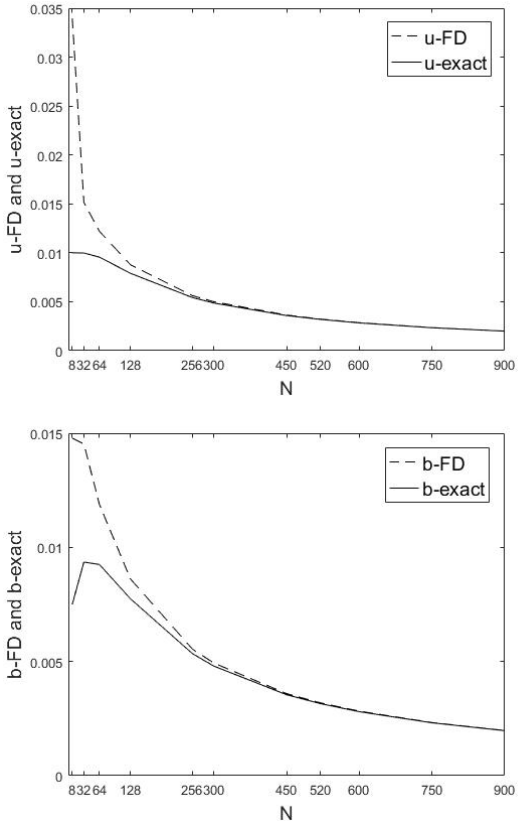

Figure 2.2: Case 1: Grid dependence on comparison with the exact solution, $Ha = 100$, $\alpha = 0$, $c = 0$.

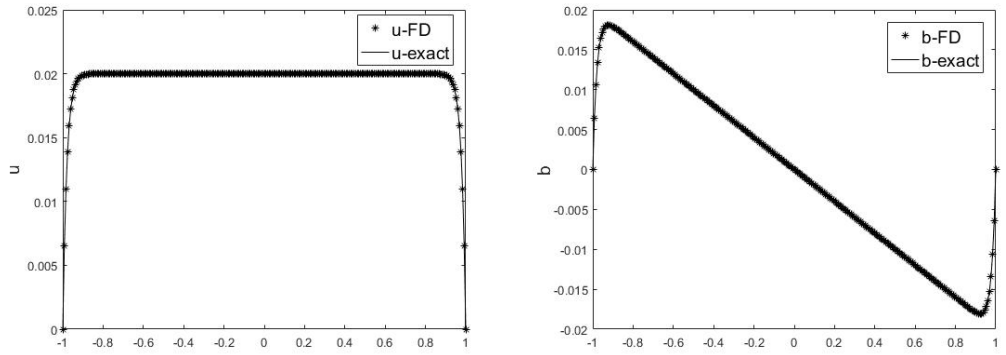

Figure 2.3: Case 1: Comparison with the exact solution, $Ha = 50$, $N = 256$, $\alpha = 0$, $c = 0$.

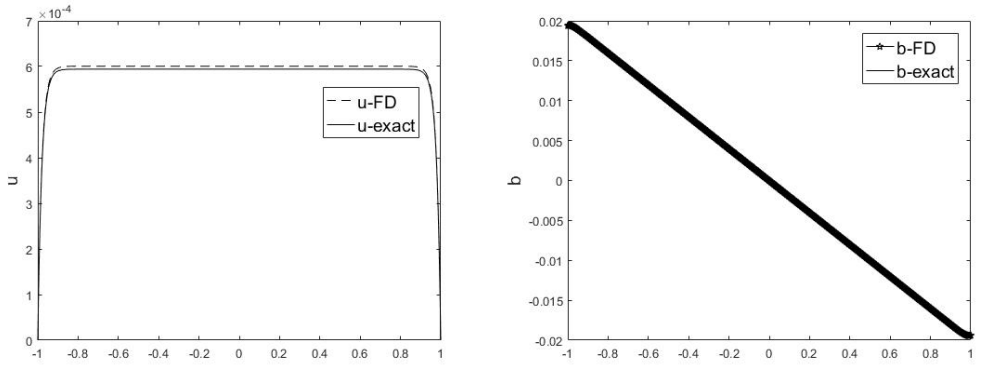

Figure 2.4: Case 2: Comparison with the exact solution, $Ha = 50$, $N = 4500$, $\alpha = 0$, $c = 2$.

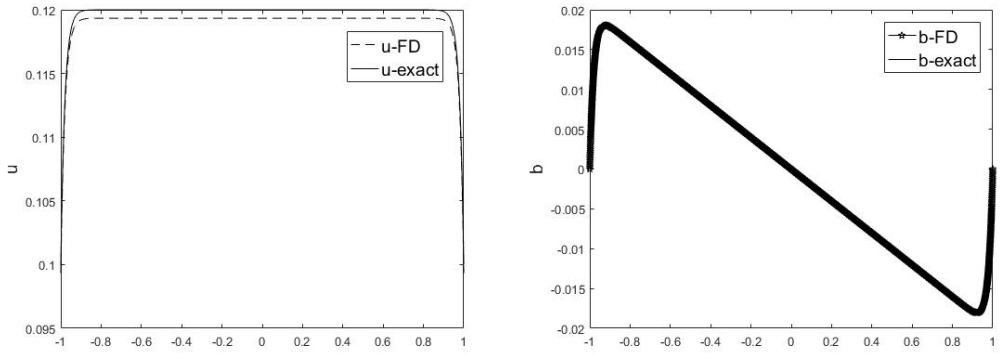

Figure 2.5: Case 3: Comparison with the exact solution, $Ha = 50$, $N = 7500$, $\alpha = 0.1$, $c = 0$.

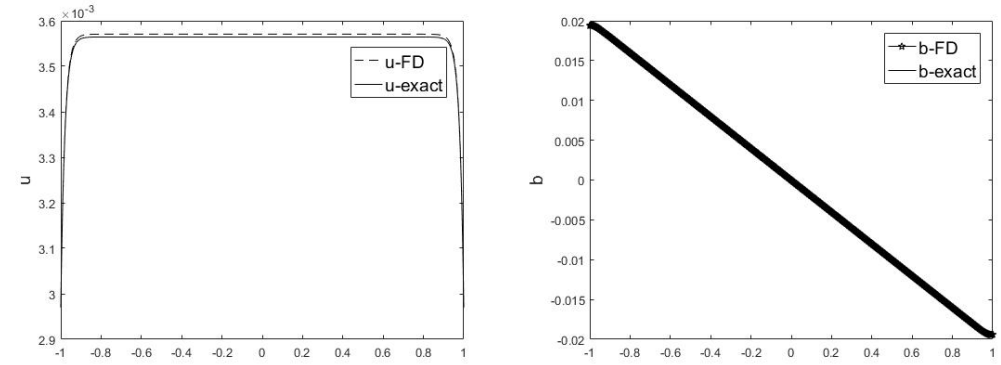

Figure 2.6: Case 4: Comparison with the exact solution, $Ha = 50$, $N = 4500$, $\alpha = 0.1$, $c = 2$.

In Figure 2.3 to Figure 2.6 we show the agreement of both the velocity and the induced magnetic field with the exact solutions. For variably conducting and slipping boundaries one needs to take quite large number of points in $[-1, 1]$ as can be seen in the Figures 2.4 to 2.6 for the cases 2, 3 and 4, respectively. It is noticed that the slipping velocity condition requires the larger N than the variably conducting boundary condition. However, when both the slip and the conductivity are effective at the end points, the number of discretization points reduces since the two effects balance each other (Case 4).

- **Case 1.** No-slip and insulated pates; $\alpha = 0$, $c = 0$.

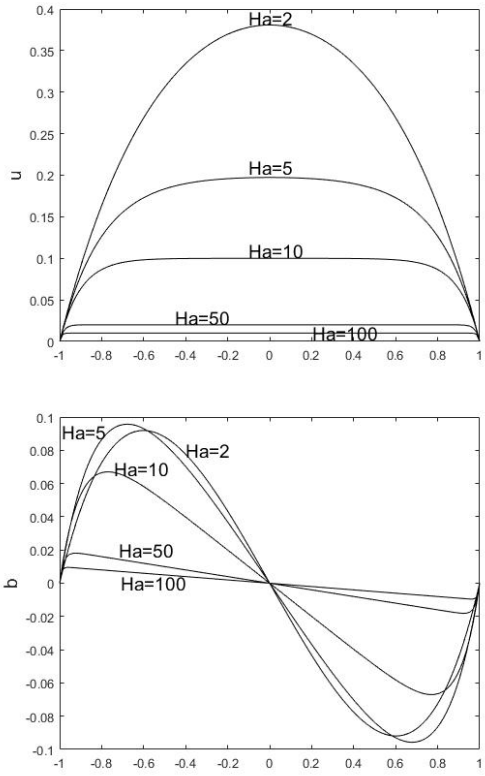

Figure 2.7: Case 1: Velocity and induced magnetic field, $\alpha = 0$, $c = 0$, $N = 256$.

It can be observed from the Figure 2.7 that as Ha increases (increasing the strength of the external magnetic field), the velocity magnitude decreases. (The well-known flattening tendency of MHD flow). The same is also true for the induced magnetic field. As Ha increases, boundary layers are seen near the end points (near the plates) for both the velocity and the induced magnetic field. Velocity is symmetric but the induced magnetic field is anti-symmetric with respect to $y = 0$ line. For the no-slip ($\alpha = 0$) and insulated (c=0) boundary (end points) the agreement of FDM solution with the exact solution can be obtained with an accuracy $\epsilon = 10^{-3}$ using $N = 256$ subintervals in $[-1, 1]$ even for large value of Ha as 100.

The agreement with the exact solution is defined with a tolerance ϵ in

$$\max_{1 \leqslant i \leqslant n} |u^i_{FD} - u^i_{exact}| < \epsilon \quad \text{and} \quad \max_{1 \leqslant i \leqslant n} |b^i_{FD} - b^i_{exact}| < \epsilon.$$

- **Case 2:** No-slip and variably conducting plates; $\alpha = 0$, $c = 0 - 10$.

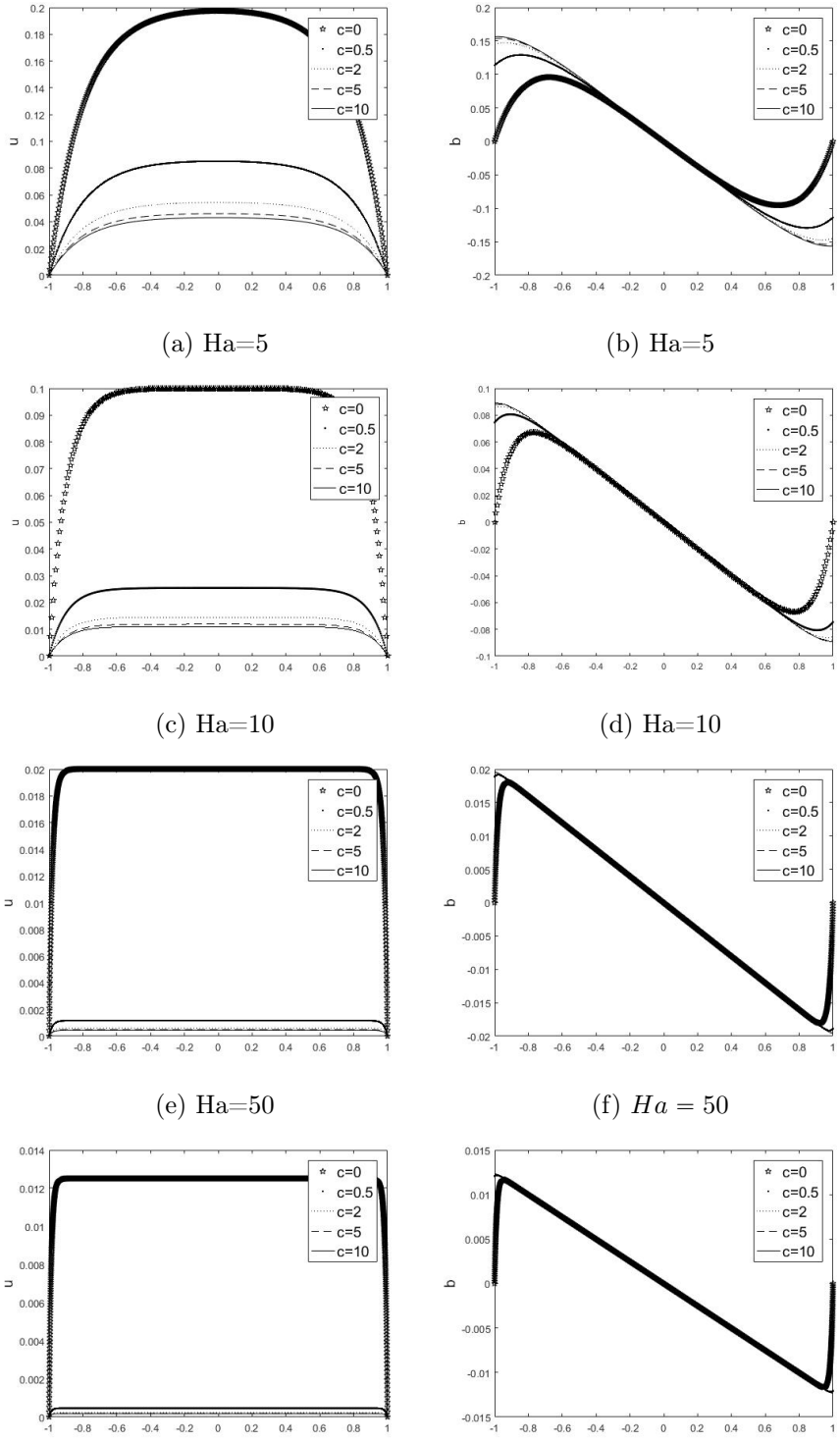

(a) Ha=5 (b) Ha=5

(c) Ha=10 (d) Ha=10

(e) Ha=50 (f) $Ha = 50$

(g) $Ha = 80$ (h) $Ha = 80$

Figure 2.8: Case 2: Velocity and induced magnetic field, $\alpha = 0$, (a),(b) $N = 450$, (c),(d) $N = 4500$, (e),(f),(g),(h) $N = 7500$.

One can notice from the Figure 2.8 that when the boundary points change from being insulated to perfectly conducting, one needs to take more discretized points in the interval [-1,1] to achieve the same accuracy $\epsilon = 10^{-3}$. As Ha increases, the velocity magnitude decreases as in the Case 1, and the flow flattens in the channel core. With increasing Hartmann number flow exhibits thin boundary layers near the Hartmann walls (plates). The induced magnetic field b reduces to zero when $c = 0$ at the end points trying to form boundary layers near the plates as Ha increases. But, when c increases, the curve of b becomes perpendicular to the end points (to the plates) $y = \pm 1$. This orthogonality behavior of b is weakened with a further increase of Ha.

- **Case 3:** Insulated but slipping plates; $c = 0$, $\alpha = 0 - 0.2$.

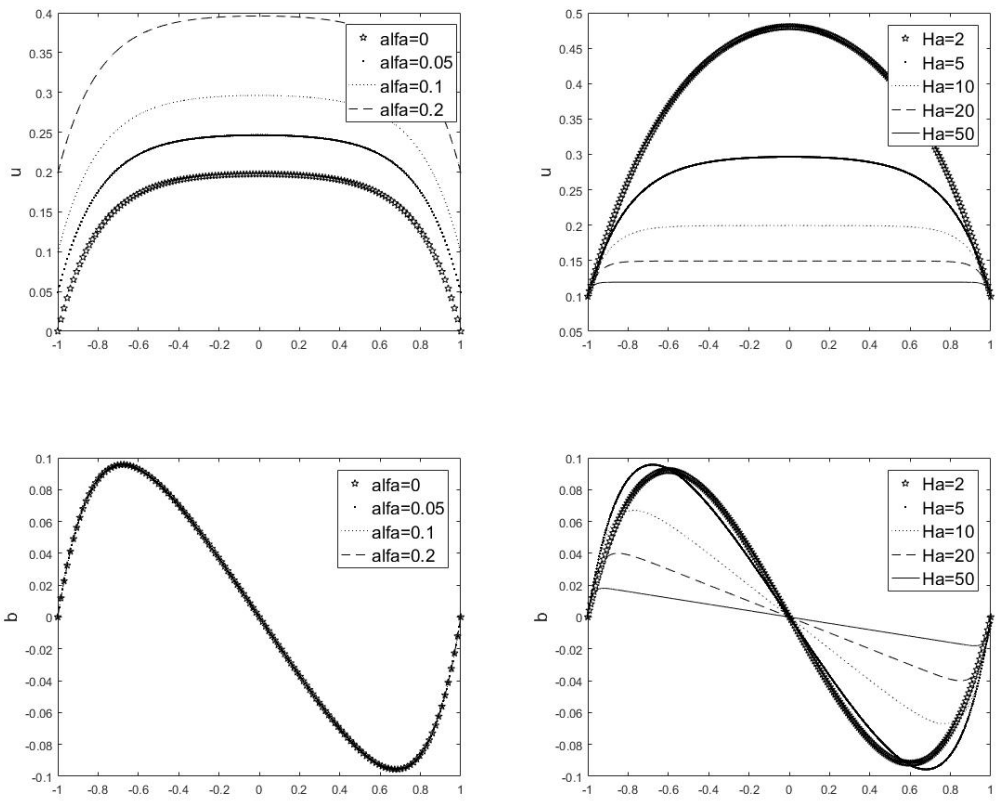

(a) (b)

Figure 2.9: Case 3: Velocity and induced magnetic field, $c = 0$, (a) Ha=5, $N = 750$ (b) $\alpha = 0.1$, $N = 7500$.

Figure 2.9 shows that as α increases, the velocity magnitude increases as noticed from Figure 2.9 (a). α increase has not much of an effect on the induced magnetic field b. Slipping velocity slightly retards the boundary layer formation as Ha increases which can be seen comparing Figure 2.7 and Figure 2.9 (b). Again for the slipping velocity case at the boundary points we need more discretized points for achieving the accuracy $\epsilon = 10^{-3}$.

- **Case 4:** Slipping and variably conducting plates; $c = 1, 10$; $\alpha = 0.05, 0.1$.

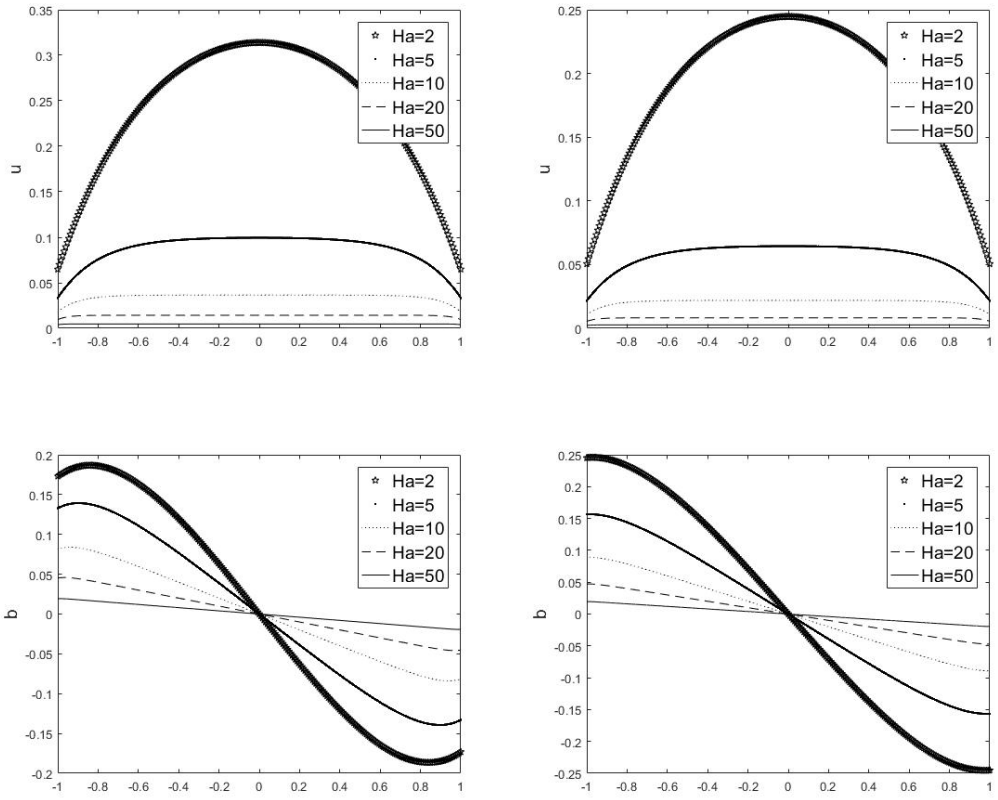

(a) c=1 (b) c=10

Figure 2.10: Case 4: Velocity and induced magnetic field, $N = 4500$, $\alpha = 0.1$.

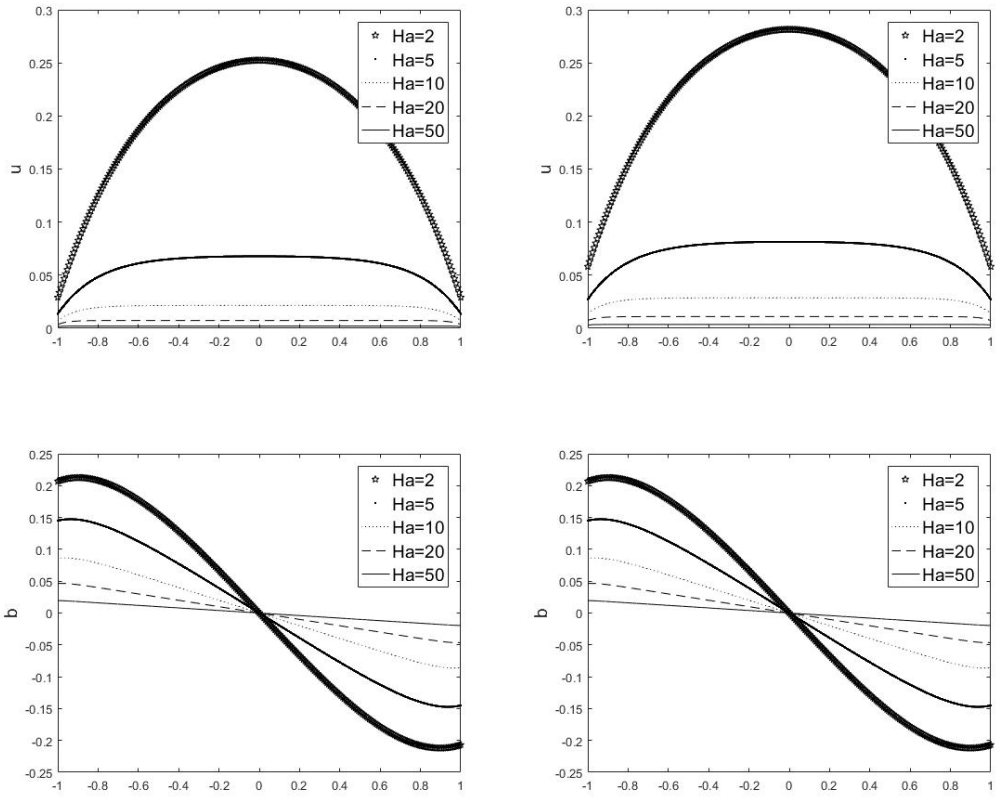

(a) $\alpha = 0.05$ (b) $\alpha = 0.1$

Figure 2.11: Case 4: Velocity and induced magnetic field, $c = 2$, $N = 4500$.

Figure 2.10 and 2.11 show that as the slip length α is kept fixed and the conductivity parameter c increases, the velocity magnitude drops for all values of Ha. Slip length α does not effect the behavior of induced magnetic field b for a fixed conductivity parameter c. As c increases for a fixed α, b becomes perpendicular to the plates (nearly perfectly conducting plates). As the slip length α is taken fixed and the conductivity parameter c increases, the induced magnetic field magnitude increases for small values of Ha whereas this magnetic field increase is not seen for larger values of Ha. As the conductivity parameter c is taken fixed and the slip length α increases, the velocity magnitude increases for small values of Ha whereas this magnitude increase is weakened for larger values of Hartmann number.

2.5 Volumetric flow rate

Knowing the velocity distribution across the channel, the volumetric flow rate can be calculated by an integration. The dimensionless flow rate computed from the exact solution is given by [10] for the Case 1 and the Case 2 as

$$Q_{1,2} = \int_{-1}^{1} u(y)dy = 2\hat{u}\left[1 - \frac{1}{Ha}\tanh(Ha)\right] \tag{2.14}$$

where $\hat{u}$ is defined in the Equation (2.4). The volumetric flow rates for the Case 3 and the Case 4 are also derived by using the exact solutions (2.7)-(2.9). Thus, the volumetric flow rate for the most general form of the exact solution is given as

$$Q_{3,4} = \int_{-1}^{1} u(y)dy = 2\tilde{u}\left[\frac{\sinh(Ha)}{Ha} - \alpha Ha\sinh(Ha) - \cosh(Ha)\right] \tag{2.15}$$

which covers all the cases, Case 1 to Case 4.

Composite Trapezoidal rule is used to find the volumetric flow rate Q from FDM results. So, we get the approximate value of the volumetric flow rate denoted by Q_{app} as

$$Q_{app} = \int_{-1}^{1} u(y)dy = h\sum_{j=2}^{N} u_j + \frac{h}{2}\left(u_1 + u_{N+1}\right) \tag{2.16}$$

where $h = \frac{2}{N}$ and N is the number of subintervals. Then, the results are tabulated and compared with the exact values of Q.

Table 2.1: Approximate and exact volumetric flow rates for Case 1 and Case 2 with $N = 4500$

	Case 1 ($\alpha = 0$, $c = 0$)		Case 2 ($\alpha = 0$, $c = 2$)	
Ha	Q_{app}	Q_1	Q_{app}	Q_2
2	0.5373	0.5373	0.3132	0.313
5	0.32	0.32	0.0874	0.0873
10	0.18	0.18	0.0258	0.0257
20	0.095	0.095	0.007	0.007
50	0.0392	0.0392	0.0012	0.0012

Table 2.2: Approximate and exact volumetric flow rates for Case 3 and Case 4 with $N = 7500$

	Case 3 ($\alpha = 0.1$, $c = 0$)		Case 4 ($\alpha = 0.1$, $c = 2$)	
Ha	Q_{app}	Q_3	Q_{app}	Q_4
2	0.7357	0.7373	0.4297	0.4296
5	0.5162	0.52	0.1419	0.1418
10	0.3725	0.38	0.0543	0.0543
20	0.2941	0.295	0.0216	0.0216
50	0.2379	0.2392	0.0071	0.0071

Table 2.3: Approximate volumetric flow rates for Case 3 and Case 4 with $N = 7500$

	$Ha = 5$		$Ha = 10$	
	Case 3 ($c = 0$)	Case 4 ($c = 2$)	Case 3 ($c = 0$)	Case 4 ($c = 2$)
α	Q_{app}	Q_{app}	Q_{app}	Q_{app}
0	0.32	0.0874	0.18	0.0258
0.05	0.4199	0.1146	0.2798	0.0401
0.1	0.5162	0.1419	0.3725	0.0543
0.2	0.7196	0.1964	0.5791	0.0829

Table 2.4: Approximate volumetric flow rates for Case 2 and Case 4 with $N = 7500$

$Ha = 5$		
c	Case 2 ($\alpha = 0$) Q_{app}	Case 4 ($\alpha = 0.1$) Q_{app}
0	0.32	0.5162
0.5	0.1391	0.2229
2	0.0874	0.1419
5	0.0739	0.1201
10	0.0691	0.1122

One can see from Table 2.1 to Table 2.4 that, the volumetric flow rates obtained as the slip length α and the conductivity parameter c are kept fixed and Ha increases, the volumetric flow rate decreases for each Case since velocity magnitude drops. The well agreement of the FDM solution values with the exact solution values is seen for the Cases 1 and 2. An increase in the wall conductivity decreases the volumetric flow rate. An increase in the slip length naturally increases the volumetric flow rate since it increases the velocity magnitude.

As a conclusion we see that as Ha increases, both the velocity and the induced magnetic field magnitudes decrease. As Ha increases, boundary layers are formed near the plates (Hartmann layers). Conductivity parameter $0 \leqslant c < \infty$ gives induced magnetic field profiles between the insulated and perfectly conducting plates. The increase in the slip length increases the velocity magnitude which is weakened for large values of Ha. For a fixed slip length α, the increase in the conductivity parameter c causes a drop in the flow but increases induced current magnitude which is weakened for large Ha. The number of subintervals in the FDM discretization needs to be increased for increasing values of the slip length and the conductivity parameter.

CHAPTER 3

2D MHD CHANNEL FLOW (MHD FLOW IN A RECTANGULAR DUCT)

In this chapter, the MHD flow of an electrically conducting fluid is considered in a long channel (pipe) of rectangular cross-section along with the z-axis. The fluid is driven by a pressure gradient along the z-axis. The flow is steady, laminar, fully-developed and is influenced by an external magnetic field applied perpendicular to the channel axis. So, the velocity field $\vec{V} = (0, 0, V)$ and the magnetic field $\vec{B} = (0, B_0, B)$ have only channel-axis components V and B depending only on the plane coordinates x and y on the cross-section of the channel which is a rectangular duct as shown in the following figure.

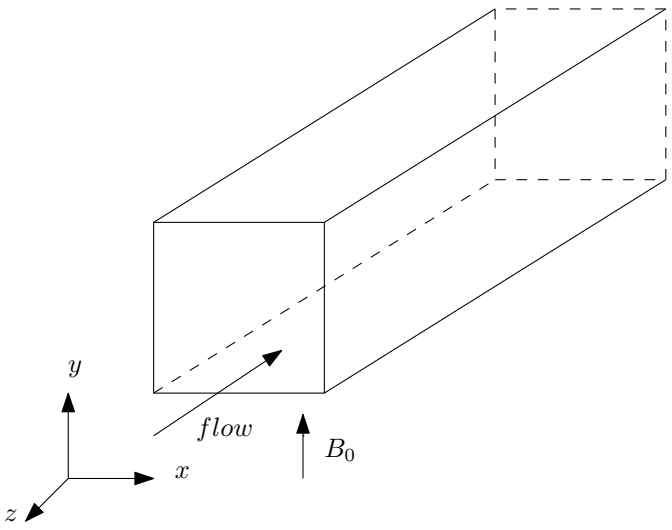

Figure 3.1: MHD Rectangular duct flow

The governing MHD equations derived in the first chapter and given by the Equations (1.21) with the boundary conditions (1.24) are solved by using the

finite difference method (FDM). Several type of boundary conditions such as slip or no-slip velocity $V(x, y)$ and conducting, insulated or partly conducting/partly insulated side walls for $B(x, y)$ are considered. The numerical solutions for each case of boundary conditions are simulated in terms of equivelocity contours and current lines. The effects of the slip and the wall conductivities on the behavior of the velocity V and the induced magnetic field B are discussed. Then, the numerical results obtained from the FDM discretized equations and the exact solution values [4] are shown on the same figure for no-slip and insulated walls to see the coincidence with the exact results. Also, the accuracy 10^{-2} is obtained for both the velocity V and the induced magnetic field B when compared with the available exact solution.

3.1 Problem Formulation

The steady, laminar, fully-developed flow of an incompressible, viscous, electrically conducting fluid is considered in a long channel of rectangular cross-section (duct). The pipe axis is along the z-axis and there is an external magnetic field applied perpendicular to the y-axis. The governing equations of 2D MHD flow in a rectangular duct are defined by

$$\begin{aligned} &\nabla^2 V + Ha\frac{\partial B}{\partial y} = -1 \\ &\qquad\qquad\qquad\qquad \text{in} \quad \Omega \\ &\nabla^2 B + Ha\frac{\partial V}{\partial y} = 0 \end{aligned} \tag{3.1}$$

with the new notations V and B instead of the notations u and b given in the Equation (1.21) for the velocity and the induced magnetic field, respectively. Here, Ha is the Hartmann number and $\Omega = \{-1 \leqslant x \leqslant 1, -1 \leqslant y \leqslant 1\}$ with the most general type of boundary conditions

$$\begin{aligned} &V \pm \alpha\frac{\partial V}{\partial y} = 0, \quad B \pm c_1\frac{\partial B}{\partial y} = 0 \quad \text{when} \quad y = \pm 1 \\ &V \pm \alpha\frac{\partial V}{\partial x} = 0, \quad B \pm c_2\frac{\partial B}{\partial x} = 0 \quad \text{when} \quad x = \pm 1. \end{aligned} \tag{3.2}$$

Here, the constants α, c_1 and c_2 are used to denote the slipping length of the velocity and the conductivity parameters for the Hartmann walls (perpendicular to the applied magnetic field) and the side walls (parallel to the applied magnetic field), respectively. Thus, $c_k \to 0$ corresponds to electrically insulating walls and $c_k \to \infty$ to electrically perfectly conducting walls for $k = 1, 2$. Also, $\alpha = 0$ indicates that we have no-slip duct walls.

3.2 FDM Solution of 2D MHD Flow Equations with Different types of Wall Conductivities

- **Case 1.**

For the first case, we choose the conductivity parameter $c_1 = c_2 = 0$ and the slipping length $\alpha = 0$ on $\partial\Omega$. So, the problem (3.1) with the boundary conditions $V = 0$ and $B = 0$ is going to be solved for this case. Physically, it shows the no-slip and insulated walls.

Firstly, the substitutions $\Phi = V + B$ and $\Psi = V - B$ are used to make the given equations in (3.1) decoupled. Adding and subtracting these equations, we obtain

$$\nabla^2(V + B) + Ha\frac{\partial(V + B)}{\partial y} = -1$$
$$\nabla^2(V - B) - Ha\frac{\partial(V - B)}{\partial y} = -1$$

which results in two decoupled convection-diffusion equations with the new variables

$$\begin{aligned} \nabla^2\Phi + Ha\frac{\partial\Phi}{\partial y} &= -1 \\ &\text{in} \quad \Omega \\ \nabla^2\Psi - Ha\frac{\partial\Psi}{\partial y} &= -1 \end{aligned} \tag{3.3}$$

and the boundary conditions become

$$\Phi = 0 \quad \text{and} \quad \Psi = 0 \quad \text{on} \quad \partial\Omega. \tag{3.4}$$

Now, the Equations in (3.3) are going to be solved by using central finite difference for the Laplacian operator ∇^2 and forward finite difference for $\dfrac{\partial}{\partial y}$ to find Φ and Ψ, numerically. Then, the original variables (the velocity and the induced magnetic field)

$$V = \frac{\Phi + \Psi}{2} \quad \text{and} \quad B = \frac{\Phi - \Psi}{2} \tag{3.5}$$

can be obtained numerically. Thus, by taking equal mesh sizes in both x- and y-directions as $\Delta x = \Delta y = h$, we get

$$\frac{\Phi_{i+1,j} - 2\Phi_{i,j} + \Phi_{i-1,j}}{h^2} + \frac{\Phi_{i,j+1} - 2\Phi_{i,j} + \Phi_{i,j-1}}{h^2} + Ha\frac{\Phi_{i,j+1} - \Phi_{i,j}}{h} = -1$$

$$\frac{\Psi_{i+1,j} - 2\Psi_{i,j} + \Psi_{i-1,j}}{h^2} + \frac{\Psi_{i,j+1} - 2\Psi_{i,j} + \Psi_{i,j-1}}{h^2} - Ha\frac{\Psi_{i,j+1} - \Psi_{i,j}}{h} = -1$$

where $i, j = 2, \ldots, N$. After multiplying both sides of the above equations by h^2 and rearranging the terms, we obtain the discretized systems

$$\begin{aligned} &\Phi_{i+1,j} - (4 + h(Ha))\Phi_{i,j} + \Phi_{i-1,j} + (1 + h(Ha))\Phi_{i,j+1} + \Phi_{i,j-1} = -h^2 \\ &\Psi_{i+1,j} - (4 - h(Ha))\Psi_{i,j} + \Psi_{i-1,j} + (1 - h(Ha))\Psi_{i,j+1} + \Psi_{i,j-1} = -h^2 \end{aligned} \tag{3.6}$$

where $i, j = 2, \ldots, N$ and N denotes the number of intervals for both of the sides in x- and y-directions. By the scheme obtained in (3.6), one can see that the number of resulting linear equations depends on N, and namely we have the coefficient matrices of size $M \times M$ for both $\Phi_{i,j}$ and $\Psi_{i,j}$ where $M = (N-1)^2$. Let C and D be these coefficient matrices for the unknown vectors Φ and Ψ which include the unknowns $\Phi_{i,j}$ and $\Psi_{i,j}$, respectively.

Then, for a general N we have the following matrix-vector systems for the unknowns $\Phi_{i,j}$ and $\Psi_{i,j}$ when the system (3.6) is used.

- **For $\Phi_{i,j}$:**

We have the system

$$C\Phi = v$$

where Φ is the unknown vector of size $M \times 1$ given by

$$\Phi = \begin{bmatrix} \Phi_{2,2} & \Phi_{2,3} & \cdots & \Phi_{2,N} & \cdots & \Phi_{N,2} & \Phi_{N,3} & \cdots & \Phi_{N,N} \end{bmatrix}^{\mathsf{T}}.$$

The vector v of size $M \times 1$ is

$$v = \begin{bmatrix} -h^2 & -h^2 & -h^2 & \cdots & -h^2 & -h^2 \end{bmatrix}^{\mathsf{T}},$$

and the coefficient matrix C of size $M \times M$ is given by

$$C = \begin{bmatrix} A & I_{N-1} & 0 & 0 & 0 & 0 & \cdots & 0 \\ I_{N-1} & A & I_{N-1} & 0 & 0 & 0 & \cdots & 0 \\ 0 & I_{N-1} & A & I_{N-1} & 0 & 0 & \cdots & 0 \\ \vdots & \vdots & \ddots & \ddots & \ddots & \vdots & \vdots & \vdots \\ \vdots & \vdots & \vdots & \ddots & \ddots & \ddots & \vdots & \vdots \\ \vdots & \vdots & \vdots & \vdots & \ddots & \ddots & \ddots & \vdots \\ 0 & \cdots & 0 & 0 & 0 & I_{N-1} & A & I_{N-1} \\ 0 & \cdots & 0 & 0 & 0 & 0 & I_{N-1} & A \end{bmatrix}$$

where the matrix A of size $(N-1) \times (N-1)$ for the scheme obtained in the Equation (3.6) is given as

$$A = \begin{bmatrix} -4-hHa & 1+hHa & 0 & 0 & 0 & \cdots & 0 \\ 1 & -4-hHa & 1+hHa & 0 & 0 & \cdots & 0 \\ 0 & 1 & -4-hHa & 1+hHa & 0 & \cdots & 0 \\ \vdots & \vdots & \vdots & \vdots & \vdots & \vdots & \vdots \\ \vdots & \vdots & \vdots & \vdots & \vdots & \vdots & \vdots \\ 0 & \vdots & \vdots & \vdots & \vdots & \vdots & 0 \\ 0 & \cdots & 0 & 0 & 1 & -4-hHa & 1+hHa \\ 0 & \cdots & 0 & 0 & 0 & 1 & -4-hHa \end{bmatrix}$$

when the forward finite difference is used for the first order derivatives.

- **For $\Psi_{i,j}$:**

We have the system

$$D\Psi = v$$

where Ψ is the unknown vector of size $M \times 1$ given by

$$\Psi = \begin{bmatrix} \Psi_{2,2} & \Psi_{2,3} & \cdots & \Psi_{2,N} & \cdots & \Psi_{N,2} & \Psi_{N,3} & \cdots & \Psi_{N,N} \end{bmatrix}^{\mathsf{T}}.$$

The vector v of size $M \times 1$ is

$$v = \begin{bmatrix} -h^2 & -h^2 & -h^2 & \cdots & -h^2 & -h^2 \end{bmatrix}^{\mathsf{T}}$$

and the coefficient matrix D of size $M \times M$ is given by

$$D = \begin{bmatrix} \tilde{A} & I_{N-1} & 0 & 0 & 0 & 0 & \cdots & 0 \\ I_{N-1} & \tilde{A} & I_{N-1} & 0 & 0 & 0 & \cdots & 0 \\ 0 & I_{N-1} & \tilde{A} & I_{N-1} & 0 & 0 & \cdots & 0 \\ \vdots & \vdots & \ddots & \ddots & \ddots & \vdots & \vdots & \vdots \\ \vdots & \vdots & \vdots & \ddots & \ddots & \ddots & \vdots & \vdots \\ 0 & \vdots & \vdots & \vdots & \ddots & \ddots & \ddots & 0 \\ 0 & \cdots & 0 & 0 & \vdots & I_{N-1} & \tilde{A} & I_{N-1} \\ 0 & \cdots & 0 & 0 & 0 & 0 & I_{N-1} & \tilde{A} \end{bmatrix}$$

where the matrix $\tilde{A}$ of size $(N-1) \times (N-1)$ for the scheme obtained in the Equation (3.6) is as follows

$$\tilde{A} = \begin{bmatrix} -4+hHa & 1-hHa & 0 & 0 & 0 & \cdots & 0 \\ 1 & -4+hHa & 1-hHa & 0 & 0 & \cdots & 0 \\ 0 & 1 & -4+hHa & 1-hHa & 0 & \cdots & 0 \\ \vdots & \vdots & \vdots & \vdots & \vdots & \vdots & \vdots \\ \vdots & \vdots & \vdots & \vdots & \vdots & \vdots & \vdots \\ 0 & \vdots & \vdots & \vdots & \vdots & \vdots & 0 \\ 0 & \cdots & 0 & 0 & 1 & -4+hHa & 1-hHa \\ 0 & \cdots & 0 & 0 & 0 & 1 & -4+hHa \end{bmatrix}.$$

One can also use the central finite differences for both ∇^2 and $\dfrac{\partial}{\partial y}$ to find Φ and Ψ, numerically. Then the discretized equations become

$$\begin{aligned}
&\Phi_{i+1,j} - 4\Phi_{i,j} + \Phi_{i-1,j} + (1 + \frac{h}{2}Ha)\Phi_{i,j+1} + (1 - \frac{h}{2}Ha)\Phi_{i,j-1} = -h^2 \\
&\Psi_{i+1,j} - 4\Psi_{i,j} + \Psi_{i-1,j} + (1 - \frac{h}{2}Ha)\Psi_{i,j+1} + (1 + \frac{h}{2}Ha)\Psi_{i,j-1} = -h^2
\end{aligned} \tag{3.7}$$

where $i, j = 2, \ldots, N$. The resulting $C\Phi = v$ and $D\Psi = v$ systems change in the A and $\tilde{A}$ matrices only as

$$A = \begin{bmatrix}
-4 & 1+\frac{hHa}{2} & 0 & 0 & 0 & 0 & \cdots & 0 \\
1-\frac{hHa}{2} & -4 & 1+\frac{hHa}{2} & 0 & 0 & 0 & \cdots & 0 \\
0 & 1-\frac{hHa}{2} & -4 & 1+\frac{hHa}{2} & 0 & 0 & \cdots & 0 \\
\vdots & \vdots & \ddots & \ddots & \ddots & \vdots & \vdots & \vdots \\
\vdots & \vdots & \vdots & \ddots & \ddots & \ddots & \vdots & \vdots \\
0 & \vdots & \vdots & \vdots & \ddots & \ddots & \ddots & 0 \\
0 & \cdots & 0 & 0 & 0 & 1-\frac{hHa}{2} & -4 & 1+\frac{hHa}{2} \\
0 & \cdots & 0 & 0 & 0 & 0 & 1 & -4
\end{bmatrix}$$

and

$$\tilde{A} = \begin{bmatrix} -4 & 1-\frac{hHa}{2} & 0 & 0 & 0 & 0 & \cdots & 0 \\ 1+\frac{hHa}{2} & -4 & 1-\frac{hHa}{2} & 0 & 0 & 0 & \cdots & 0 \\ 0 & 1+\frac{hHa}{2} & -4 & 1-\frac{hHa}{2} & 0 & 0 & \cdots & 0 \\ \vdots & \vdots & \ddots & \ddots & \ddots & \vdots & \vdots & \vdots \\ \vdots & \vdots & \vdots & \ddots & \ddots & \ddots & \vdots & \vdots \\ 0 & \vdots & \vdots & \vdots & \ddots & \ddots & \ddots & 0 \\ 0 & \cdots & 0 & 0 & 0 & 1+\frac{hHa}{2} & -4 & 1-\frac{hHa}{2} \\ 0 & \cdots & 0 & 0 & 0 & 0 & 1+\frac{hHa}{2} & -4 \end{bmatrix}.$$

The discretized system of equations $C\Phi = v$ and $D\Psi = v$ resulting from both systems (3.6) and (3.7) are solved for Φ and Ψ vectors and then the velocity V and the induced magnetic field B are obtained through the relation (3.5).

For the other cases of boundary conditions, we are going to solve the Equations (3.1) as a whole with the most general boundary conditions (3.2). Firstly, discretizing the MHD equations as a whole by central finite differences for ∇^2 and $\dfrac{\partial}{\partial y}$ we obtain

$$\frac{V_{i+1,j} - 2V_{i,j} + V_{i-1,j}}{h^2} + \frac{V_{i,j+1} - 2V_{i,j} + V_{i,j-1}}{h^2} + Ha\frac{B_{i,j+1} - B_{i,j-1}}{2h} = -1$$

$$\frac{B_{i+1,j} - 2B_{i,j} + B_{i-1,j}}{h^2} + \frac{B_{i,j+1} - 2B_{i,j} + B_{i,j-1}}{h^2} - Ha\frac{V_{i,j+1} - V_{i,j-1}}{2h} = 0$$

where N is the number of nodes taken on each side, $h = \dfrac{2}{N}$ is the step size. Multiplying each side of the above equations by h^2 and rearranging the terms

give

$$V_{i+1,j} - 4V_{i,j} + V_{i-1,j} + V_{i,j+1} + V_{i,j-1} + \frac{h(Ha)}{2}\left(B_{i,j+1} - B_{i,j-1}\right) = -h^2$$

$$B_{i+1,j} - 4B_{i,j} + B_{i-1,j} + B_{i,j+1} + B_{i,j-1} + \frac{h(Ha)}{2}\left(V_{i,j+1} - V_{i,j-1}\right) = 0 \tag{3.8}$$

where $i, j = 2, \ldots, N$. Also, the domain of the problem with these boundary conditions is illustrated as follows.

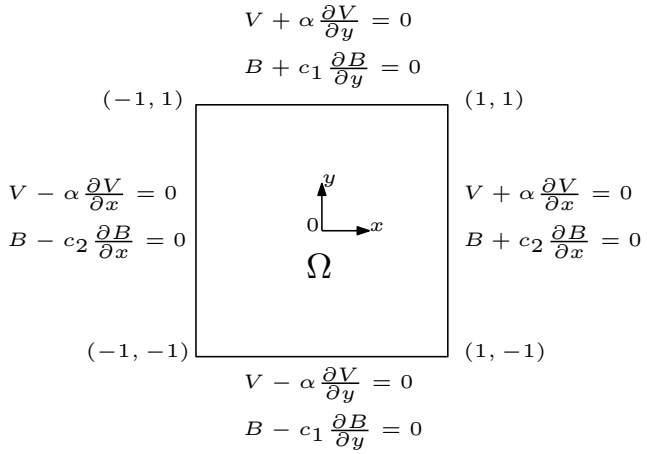

Figure 3.2: The domain (duct) and the boundary conditions

The forward finite difference is used on the sides $x = -1$ and $y = -1$ whereas the backward finite difference is used on the sides $x = 1$ and $y = 1$ in order to define boundary values in terms of inner mesh point values. The discretization of the square duct is shown as in the following figure.

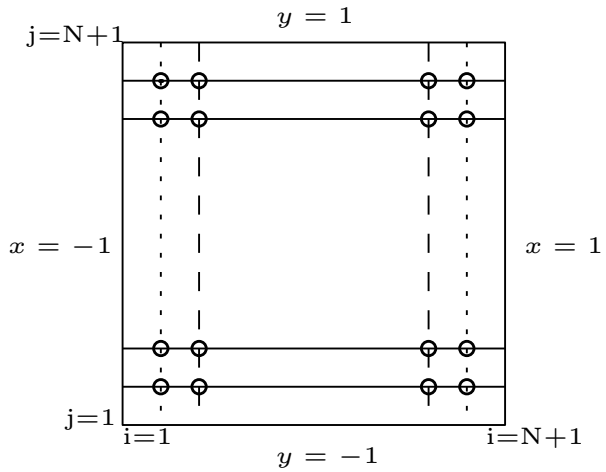

Figure 3.3: The discretization of the domain

The approximation of mixed boundary conditions are carried as follows:

When $x = -1$, $i = 1$ and $j = 1, \ldots, N+1$, we use forward FDM so that

$$V_{1,j} - \alpha \frac{V_{2,j} - V_{1,j}}{h} = 0 \quad \Rightarrow \quad V_{1,j} = \frac{\alpha}{\alpha + h} V_{2,j} \tag{3.9}$$

$$B_{1,j} - c_2 \frac{B_{2,j} - B_{1,j}}{h} = 0 \quad \Rightarrow \quad B_{1,j} = \frac{c_2}{c_2 + h} B_{2,j} \tag{3.10}$$

When $x = 1$, $i = N+1$ and $j = 1, \ldots, N+1$, we use backward FDM as

$$V_{N+1,j} + \alpha \frac{V_{N+1,j} - V_{N,j}}{h} = 0 \quad \Rightarrow \quad V_{N+1,j} = \frac{\alpha}{\alpha + h} V_{N,j} \tag{3.11}$$

$$B_{N+1,j} - c_2 \frac{B_{N+1,j} - B_{N,j}}{h} = 0 \quad \Rightarrow \quad B_{N+1,j} = \frac{c_2}{c_2 + h} B_{N,j} \tag{3.12}$$

When $y = 1$, $j = N+1$ and $i = 1, \ldots, N+1$, we use backward FDM as

$$V_{i,N+1} + \alpha \frac{V_{i,N+1} - V_{i,N}}{h} = 0 \quad \Rightarrow \quad V_{i,N+1} = \frac{\alpha}{\alpha + h} V_{i,N} \tag{3.13}$$

$$B_{i,N+1} - c_1 \frac{B_{i,N+1} - B_{i,N}}{h} = 0 \quad \Rightarrow \quad B_{i,N+1} = \frac{c_1}{c_1 + h} B_{i,N} \tag{3.14}$$

When $y = -1$, $j = 1$ and $i = 1, \ldots, N+1$, we use forward FDM as

$$V_{i,1} - \alpha \frac{V_{i,2} - V_{i,1}}{h} = 0 \quad \Rightarrow \quad V_{i,1} = \frac{\alpha}{\alpha + h} V_{i,2} \tag{3.15}$$

$$B_{i,1} - c_1 \frac{B_{i,2} - B_{i,1}}{h} = 0 \quad \Rightarrow \quad B_{i,1} = \frac{c_1}{c_1 + h} B_{i,2}. \tag{3.16}$$

Then, inserting the boundary conditions given in the Equations from (3.9) to (3.16) into the scheme (3.8) we obtain M unknowns in M equations where $M = 2(N-1)^2$ for a general N. Then, these equations are written in a matrix-vector system with the coefficient matrix Q of size $M \times M$. Thus, we have

$$Qx = w \tag{3.17}$$

where x is the unknown vector of size $M \times 1$ given by

$$x = \begin{bmatrix} V_{2,2} & B_{2,2} \cdots V_{2,N} & B_{2,N} & \cdots & V_{N,2} & B_{N,2} \cdots V_{N,N} & B_{N,N} \end{bmatrix}^{\mathsf{T}}.$$

The vector w of size $M \times 1$ is

$$w = \begin{bmatrix} -h^2 & 0 & -h^2 & 0 & \cdots & -h^2 & 0 & -h^2 & 0 \end{bmatrix}^{\mathsf{T}}.$$

The coefficient matrix Q of size $M \times M$ is a block diagonal matrix which includes two different matrices Q_1 and Q_2 of sizes $2(N-1) \times 2(N-1)$ on the diagonal block as shown below

$$Q = \begin{bmatrix} Q_1 & I_{2(N-1)} & 0 & 0 & 0 & 0 & \cdots & 0 \\ I_{2(N-1)} & Q_2 & I_{2(N-1)} & 0 & 0 & 0 & \cdots & 0 \\ 0 & I_{2(N-1)} & Q_2 & I_{2(N-1)} & 0 & 0 & \cdots & 0 \\ \vdots & \vdots & \ddots & \ddots & \ddots & \vdots & \vdots & \vdots \\ \vdots & \vdots & \vdots & \ddots & \ddots & \ddots & \vdots & \vdots \\ 0 & \vdots & \vdots & \vdots & \ddots & \ddots & \ddots & 0 \\ 0 & \cdots & 0 & 0 & \vdots & I_{2(N-1)} & Q_2 & I_{2(N-1)} \\ 0 & \cdots & 0 & 0 & 0 & 0 & I_{2(N-1)} & Q_1 \end{bmatrix}.$$

The block matrices Q_1 and Q_2 are the matrices including the Hartmann number Ha, step-size h, slipping length α and the conductivity parameters c_1, c_2 in its entries. In the coefficient matrix Q, we have the matrix Q_1 on the first and the last block of the diagonal and for the others the matrix Q_2 is repeated on the diagonal. The reason for having such a coefficient matrix Q is that we have the contributions of the boundary conditions on the sides $x = \pm 1$ and $y = \pm 1$ to the discretized points which lie on the first and the last discretized line in the domain Ω illustrated as $\cdots\cdots$ in the Figure 3.3 whereas we have only the contributions of the plates $y = \pm 1$ to the inner discretized points which lie on the lines represented as $- - -$ in the domain. For simplicity, we define some entries in these matrices as

$$L = \frac{h}{2}Ha, \quad a = \frac{\alpha}{\alpha + h}, \quad b_i = \frac{c_i}{c_i + h}, \quad \tilde{b} = b_1 + b_2$$

for $i = 1, 2$. Then the matrices Q_1 and Q_2 take the form

$$Q_1 = \begin{bmatrix}
-4+2a & -Lb_1 & 1 & L & 0 & 0 & 0 & \cdots & 0 & 0 \\
-La & -4+\tilde{b} & L & 1 & 0 & 0 & 0 & \cdots & 0 & 0 \\
1 & -L & -4+a & 0 & 1 & L & 0 & \cdots & 0 & 0 \\
-L & 1 & 0 & -4+b_2 & L & 1 & 0 & \cdots & 0 & 0 \\
\vdots & \ddots & \ddots & \ddots & \ddots & \ddots & \ddots & \ddots & \vdots & \vdots \\
\vdots & \vdots & \ddots & \ddots & \ddots & \ddots & \ddots & \ddots & \ddots & \vdots \\
0 & 0 & \vdots & 0 & 1 & -L & -4+a & 0 & 1 & L \\
0 & 0 & \vdots & 0 & -L & 1 & 0 & -4+b_2 & L & 1 \\
0 & 0 & \cdots & 0 & 0 & 0 & 1 & -L & -4+2a & Lb_1 \\
0 & 0 & \cdots & 0 & 0 & 0 & -L & 1 & La & -4+\tilde{b}
\end{bmatrix}$$

and

$$Q_2 = \begin{bmatrix} -4+a & -Lb_1 & 1 & L & 0 & 0 & 0 & \cdots & 0 & 0 \\ -La & -4+b_1 & L & 1 & 0 & 0 & 0 & \cdots & 0 & 0 \\ 1 & -L & -4 & 0 & 1 & L & 0 & \cdots & 0 & 0 \\ -L & 1 & 0 & -4 & L & 1 & 0 & \cdots & 0 & 0 \\ \vdots & \ddots & \ddots & \ddots & \ddots & \ddots & \ddots & \ddots & \vdots & \vdots \\ \vdots & \vdots & \ddots & \ddots & \ddots & \ddots & \ddots & \ddots & \ddots & \vdots \\ 0 & 0 & \vdots & 0 & 1 & -L & -4 & 0 & 1 & L \\ 0 & 0 & \vdots & 0 & -L & 1 & 0 & -4 & L & 1 \\ 0 & 0 & \cdots & 0 & 0 & 0 & 1 & -L & -4+a & Lb_1 \\ 0 & 0 & \cdots & 0 & 0 & 0 & -L & 1 & La & -4+b_1 \end{bmatrix}.$$

Finally, we obtain the unknown vector x at the discretized points from the solution of the system (3.17) by using Gaussian elimination in Matlab.

Now, from the system (3.17) we can deduce the solutions for the cases 2, 3 and 4 by only changing the values of the slip length parameter α and the conductivity parameters c_1 and c_2.

- **Case 2.**

For this case, the problem (3.1) is going to be solved with no-slip and conducting walls to see only the effect of the conductivity parameter on the behavior of the velocity V and the induced magnetic field B. Thus, we take the following boundary conditions from (3.2) with $\alpha = 0$

$$\begin{aligned} V &= 0 \quad \text{on} \quad \partial\Omega \\ B \pm c_1 \frac{\partial B}{\partial y} &= 0 \quad \text{on} \quad y = \pm 1 \\ B \pm c_2 \frac{\partial B}{\partial y} &= 0 \quad \text{on} \quad x = \pm 1. \end{aligned}$$

For simplicity, we choose the conductivity parameters equal as $c_1 = c_2 = c$ so that

$$V = 0 \quad \text{and} \quad B \pm c \frac{\partial B}{\partial n} = 0 \quad \text{on} \quad \partial\Omega. \tag{3.18}$$

Thus, the solution of this case is obtained from the system $Qx = v$ for the values $\alpha = 0$ and varying c. Then, the numerical results of discretized MHD flow equations with the boundary conditions (3.18) are simulated for several values of Hartmann number with reasonable values of conductivity parameter between insulated and perfectly conducting walls.

- **Case 3.**

Next, we consider the problem (3.1) with the boundary conditions

$$\begin{aligned} B &= 0 \quad \text{on} \quad \partial\Omega \\ V \pm \alpha \frac{\partial V}{\partial y} &= 0 \quad \text{on} \quad y = \pm 1, \quad x = \pm 1 \end{aligned} \tag{3.19}$$

to understand only the influence of the slipping length of the walls onto the solution V and B.

Then, by substituting $c_1 = c_2 = 0$ in the entries of the coefficient matrix Q, the numerical solution at the discretized points are obtained from the system $Qx = v$. Also, the results are shown in the next section for some values of slipping length with varying values of Hartmann number.

- **Case 4.**

The problem (3.1) is discussed with slipping and conducting plates (walls of the duct). So, we solve the problem with the most general type of boundary conditions given in (3.2). Again we use the same conductivity parameters as $c_1 = c_2 = c$ for varying α that

$$V \pm \alpha \frac{\partial V}{\partial n} = 0 \quad \text{and} \quad B \pm c \frac{\partial B}{\partial n} = 0 \quad \text{on} \quad \partial\Omega. \tag{3.20}$$

Thus, the system $Qx = v$ is solved with the boundary conditions (3.20). We investigate the effects of the slipping length and the wall conductivity by taking the values of the parameters as $\alpha = 0.1$ and $c = 2$. Then, the profiles of the velocity V and the induced magnetic field B are simulated for several values of Hartmann number.

- **Case 5.**

Finally, the MHD rectangular duct problem is considered with perfectly conducting no-slip Hartmann walls (the walls perpendicular to the applied magnetic field) and insulating no-slip side walls (the walls parallel to the applied magnetic field), that is

$$\begin{aligned} V(\pm 1, y) &= 0, \qquad B(\pm 1, y) = 0, \quad -1 \leqslant y \leqslant 1 \\ V(x, \pm 1) &= 0, \qquad \pm \frac{\partial B}{\partial y}|_{y=\pm 1} = 0, \quad -1 \leqslant x \leqslant 1. \end{aligned}$$

Thus, on the side walls $x = \pm 1$, we know the velocity and induced magnetic field

$$V_{1,j} = V_{N+1,j} = 0 \tag{3.21}$$

$$B_{1,j} = B_{N+1,j} = 0 \tag{3.22}$$

for $j = 1, \ldots, N+1$. Since no-slip condition is imposed for the velocity V also at $y = \pm 1$, we also have

$$V_{i,1} = V_{i,N+1} = 0 \tag{3.23}$$

for $i = 1, \ldots, N+1$. But for the induced magnetic field B, backward finite difference at $y = 1$ and forward finite difference at $y = -1$ are used for the

approximation of the derivative $\dfrac{\partial}{\partial y}$ to find the boundary values in terms of the inner values resulting in

$$B_{i,N+1} = B_{i,N}, \quad B_{i,1} = B_{i,2} \tag{3.24}$$

for $i = 1, \ldots, N+1$. Inserting these values (3.21)-(3.24) into the scheme (3.8), we obtain M unknowns in M equations where $M = 2(N-1)^2$ for a general N. Then, these equations are written in a matrix-vector system with the coefficient matrix R of size $M \times M$. So, we have

$$Rx = p$$

where x is the unknown vector of size $M \times 1$ given by

$$x = \begin{bmatrix} V_{2,2} & B_{2,2} \cdots V_{2,N} & B_{2,N} & \cdots & V_{N,2} & B_{N,2} \cdots V_{N,N} & B_{N,N} \end{bmatrix}^{\mathsf{T}}.$$

The vector p of size $M \times 1$ is

$$p = \begin{bmatrix} -h^2 & -h^2 & -h^2 & \cdots & -h^2 & -h^2 \end{bmatrix}^{\mathsf{T}},$$

and the coefficient matrix R of size $M \times M$ is given as

$$R = \begin{bmatrix} \hat{A} & I_{2(N-1)} & 0 & 0 & 0 & 0 & \cdots & 0 \\ I_{2(N-1)} & \hat{A} & I_{2(N-1)} & 0 & 0 & 0 & \cdots & 0 \\ 0 & I_{2(N-1)} & \hat{A} & I_{2(N-1)} & 0 & 0 & \cdots & 0 \\ \vdots & \vdots & \ddots & \ddots & \ddots & \vdots & \vdots & \vdots \\ \vdots & \vdots & \vdots & \ddots & \ddots & \ddots & \vdots & \vdots \\ \vdots & \vdots & \vdots & \vdots & \ddots & \ddots & \ddots & \vdots \\ 0 & \cdots & 0 & 0 & \vdots & I_{2(N-1)} & \hat{A} & I_{2(N-1)} \\ 0 & \cdots & 0 & 0 & 0 & 0 & I_{2(N-1)} & \hat{A} \end{bmatrix}$$

where the matrix $\hat{A}$ of size $2(N-1) \times 2(N-1)$ for the scheme obtained in the equation (3.8) is

$$\hat{A} = \begin{bmatrix}
-4 & -\frac{hHa}{2} & 1 & \frac{hHa}{2} & 0 & 0 & 0 & \cdots & 0 & 0 \\
0 & -3 & \frac{hHa}{2} & 1 & 0 & 0 & 0 & \cdots & 0 & 0 \\
1 & -\frac{hHa}{2} & -4 & 0 & 1 & \frac{hHa}{2} & 0 & \cdots & 0 & 0 \\
-\frac{hHa}{2} & 1 & 0 & -4 & \frac{hHa}{2} & 1 & 0 & \cdots & 0 & 0 \\
0 & 0 & \ddots & \ddots & \ddots & \ddots & \ddots & \ddots & \vdots & \vdots \\
\vdots & \vdots & \ddots & \ddots & \ddots & \ddots & \ddots & \ddots & 0 & 0 \\
0 & 0 & \vdots & 0 & 1 & -\frac{hHa}{2} & -4 & 0 & 1 & \frac{hHa}{2} \\
0 & 0 & \cdots & 0 & -\frac{hHa}{2} & 1 & 0 & -4 & \frac{hHa}{2} & 1 \\
0 & 0 & \cdots & 0 & 0 & 0 & 1 & -\frac{hHa}{2} & -4 & \frac{hHa}{2} \\
0 & 0 & \cdots & 0 & 0 & 0 & -\frac{hHa}{2} & 1 & 0 & -3
\end{bmatrix}.$$

Then, the system $Rx = p$ is solved by using Gaussian elimination from Matlab.

3.3 Numerical Results

The numerical values of the velocity V and the induced magnetic field B at the mesh points are obtained from the FDM discretized equations (3.6) or (3.7) by using forward or central differences for $\partial/\partial y$, respectively or from the whole discretized system (3.8) with central differences. To compare the approximate FDM solution obtained from the scheme (3.8) with the corresponding exact solution for the no-slip and insulated duct walls (Case 1), we use the exact solution given in [4]. The agreement is very well for $Ha = 10$ by taking only $N = 40$ intervals on each side of the duct and the convergence of FDM solution

to the exact solution is obtained with an accuracy $\epsilon = 10^{-2}$ where

$$\max_{i,j=1,\ldots,N} |V_{i,j} - V_{i,j}^{exact}| < \epsilon \quad \text{and} \quad \max_{i,j=1,\ldots,N} |B_{i,j} - B_{i,j}^{exact}| < \epsilon.$$

One the other hand, we need to increase the value of N with an increasing Hartmann number for obtaining accurate results at the mesh points since Ha increase causes convection dominance in the MHD equations. So, we use $N = 30, 40, 60, 80, 100$ with the corresponding values of $Ha = 5, 10, 30, 50, 100$. Then, the velocity and the induced magnetic field profiles are simulated for several values of Hartmann number in Figures 3.5 to 3.6.

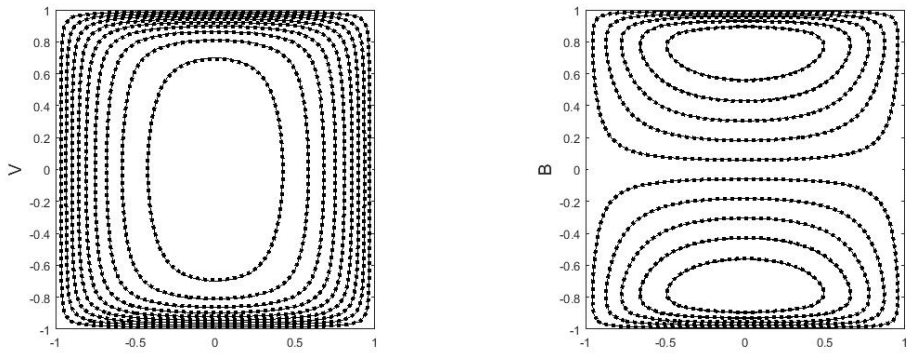

Figure 3.4: Case 1: Velocity and induced magnetic field, $Ha = 10$, $N = 40$, exact (solid), FDM (dashed).

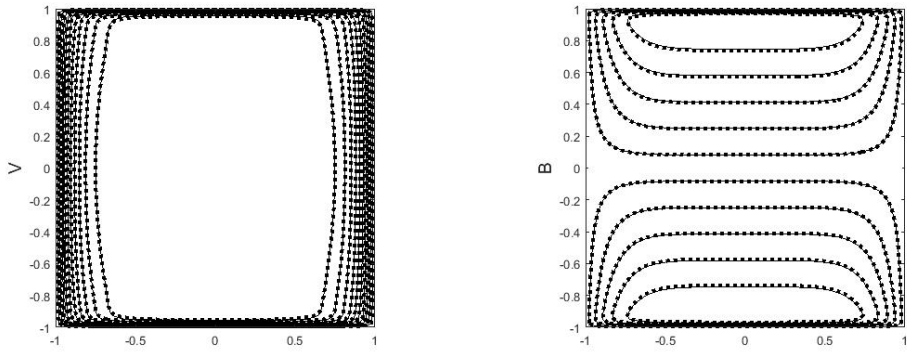

Figure 3.5: Case 1: Velocity and induced magnetic field, $Ha = 50$, $N = 80$, exact (solid), FDM (dashed).

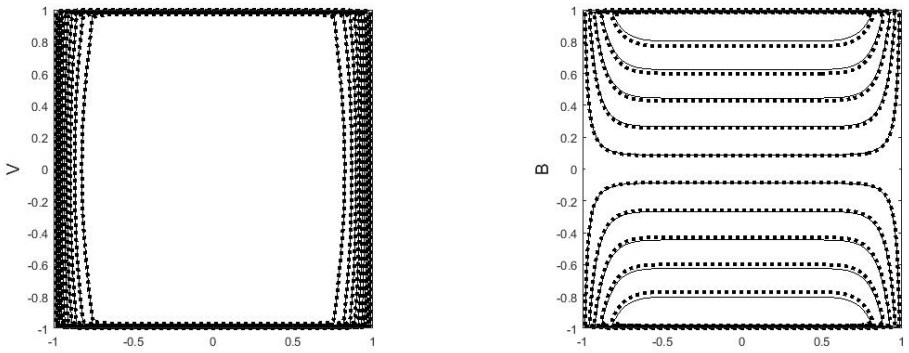

Figure 3.6: Case 1: Velocity and induced magnetic field, $Ha = 100$, $N = 100$, exact (solid), FDM (dashed).

The very well agreements of the FDM and exact solution equivelocity and equal current lines can be observed from the Figures 3.4 to 3.6 for increasing Hartmann number values.

- **Case 1.** No-slip and insulated walls; $\alpha = 0$, $c = 0$.

In Figure 3.7, the velocity and the induced magnetic field behaviors are simulated for increasing values of Hartmann number when the duct walls are electrically insulated but no-slip walls. It is noticed that one needs to take more number of discretized points N as Ha increases to achieve an accuracy of $\epsilon = 10^{-2}$. One can notice from Figure 3.7 that as Ha increases, that is, the strength of the induced magnetic field increases, both the velocity and the induced magnetic field magnitudes decrease. This is the flattening tendency of MHD flow for increasing values of Ha, [4].

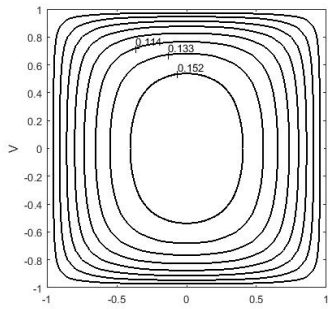

(a) $Ha = 5$, $N = 30$

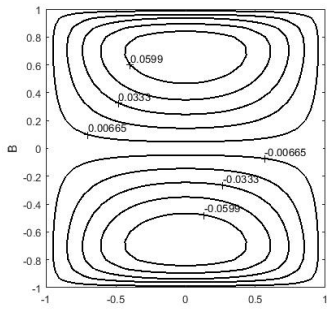

(b) $Ha = 5$, $N = 30$

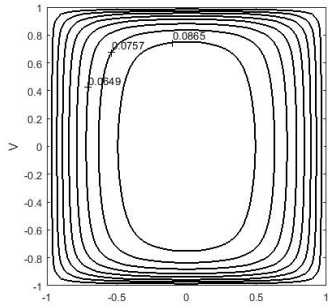

(c) $Ha = 10$, $N = 40$

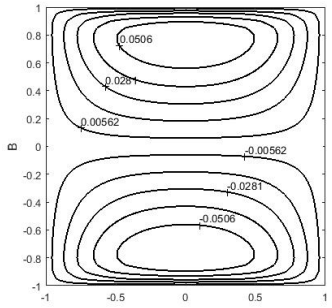

(d) $Ha = 10$, $N = 40$

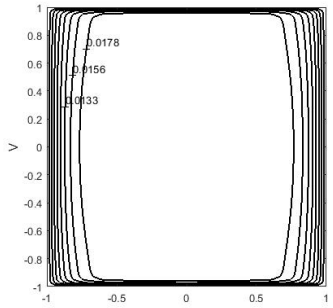

(e) $Ha = 50$, $N = 80$

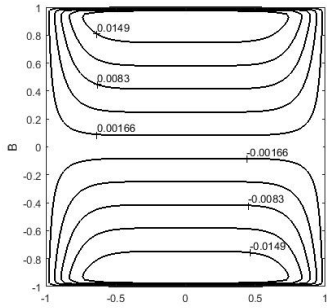

(f) $Ha = 50$, $N = 80$

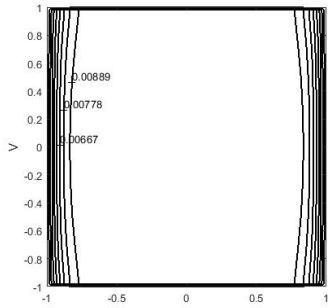

(g) $Ha = 100$, $N = 100$

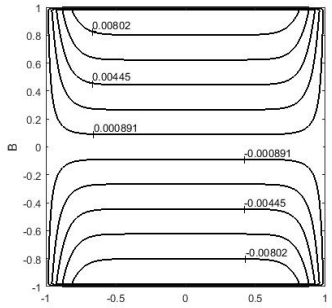

(h) $Ha = 100$, $N = 100$

Figure 3.7: Case1: Velocity and induced magnetic field.

As Ha increases, boundary layers are developed near the Hartmann walls (walls perpendicular to the applied magnetic field) for both the velocity and the induced magnetic field. Near the Hartmann walls the velocity drops sharply within the boundary layers. These layers are called the *Hartmann layers*. From the theory of boundary layers in MHD duct flow, the thickness of Hartmann layers is of order $1/Ha$ and the thickness of side layers which are also developed as Ha increases is of order $1/\sqrt{Ha}$, [4]. The fluid becomes stagnant at the center of the duct. Velocity is symmetric with respect to $x = 0$ and $y = 0$ lines and the induced magnetic field is anti-symmetric with respect to $y = 0$ line.

- **Case 2.** No-slip and variably conducting walls; $\alpha = 0$, $c = 0.5 - 10$.

Figure 3.8 shows the simulation of the velocity and the induced magnetic field for increasing values of conductivity parameter c for a fixed Hartmann number $Ha = 10$. It is seen from the figure that as the conductivity parameter c increases the velocity magnitudes decrease whereas the induced magnetic field magnitudes increase. But, the increase in the induced magnetic field magnitude becomes weak when c increases. Also, the profiles of the induced magnetic field reveal that it tries to become perpendicular to the side walls as the conductivity parameter c increases but this orthogonality is weakened for small values of c. That is, for $c \approx 10$ the side walls almost become electrically perfectly conducting.

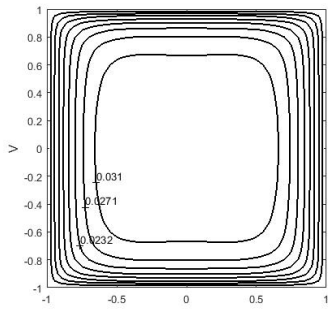

(a) $c = 0.5$

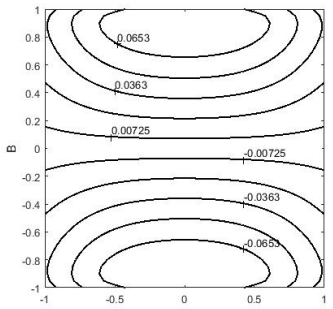

(b) $c = 0.5$

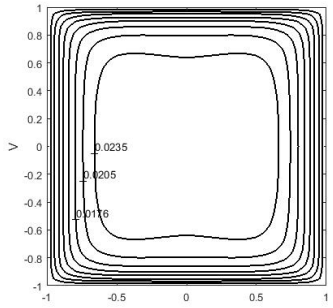

(c) $c = 1$

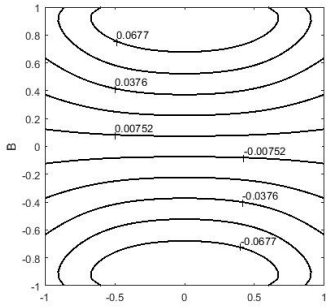

(d) $c = 1$

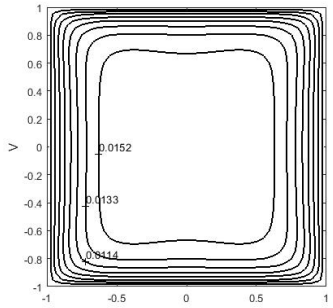

(e) $c = 5$

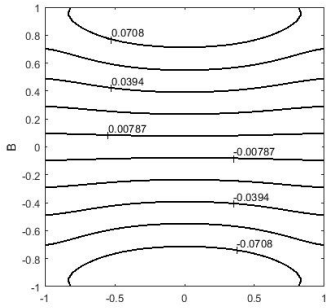

(f) $c = 5$

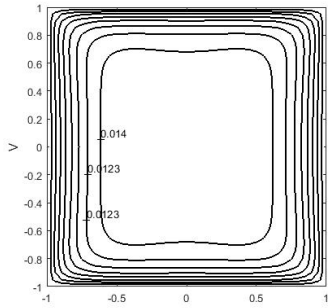

(g) $c = 10$

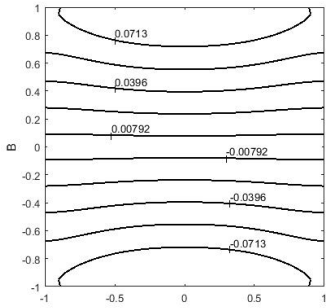

(h) $c = 10$

Figure 3.8: Case 2: Velocity and induced magnetic field for $Ha = 10$, $\alpha = 0$.

- **Case 3.** Insulated but slipping walls; $\alpha = 0.01 - 0.3$, $c = 0$.

In Figure 3.9 the profiles of the velocity and the induced magnetic field are simulated for several values of slipping parameter α. As observed from the figure, numerical results reveal that the velocity magnitudes increase when α increases. This is a theoretically known behavior, [15]. On the other hand, an increase in the slipping length causes a decrease in the induced magnetic field. As the slipping parameter α increases, the slip on the walls increases and we see much more slip on the Hartmann walls than on the side walls.

- **Case 4.** Slipping and variably conducting walls; $\alpha = 0.1$, $c = 2$.

The velocity and the induced magnetic field are presented in Figure 3.10 for varying values of Hartmann number Ha. One can see easily that the velocity and the induced magnetic field magnitudes drop as Ha increases. For a small value of Hartmann number ($Ha = 10$), the slip is seen on the Hartmann walls, which is disappeared for large values of Hartmann number ($Ha = 30, 50, 100$).

Also, it is observed from the velocity profiles that we have Hartmann layers for moderate values of Hartmann number ($Ha = 30, 50$), which is very thin for $Ha = 100$ obeying the order $1/Ha$. As Ha increases the core region increases and the fluid flows near the side walls. In addition to these, the profiles of the induced magnetic field show that the induced magnetic field becomes perpendicular to the side walls with an increase in Ha which is weakened for small values of Hartmann number such as $Ha = 10, 30$.

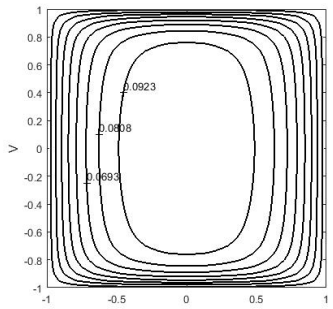

(a) $\alpha = 0.01$

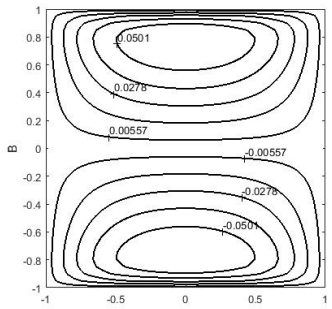

(b) $\alpha = 0.01$

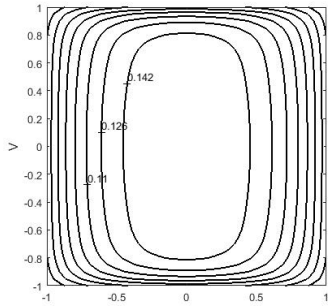

(c) $\alpha = 0.1$

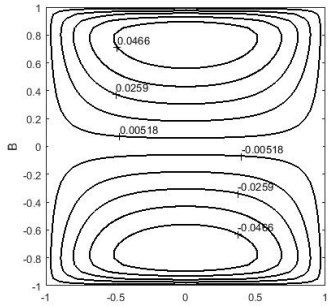

(d) $\alpha = 0.1$

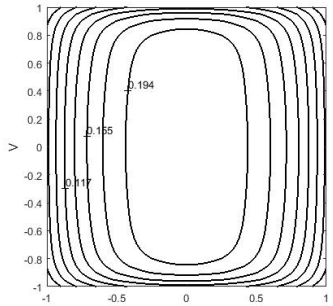

(e) $\alpha = 0.2$

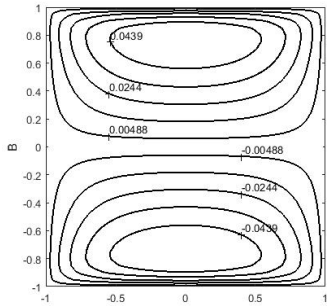

(f) $\alpha = 0.2$

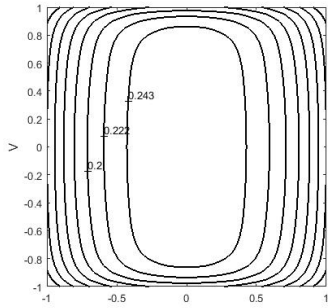

(g) $\alpha = 0.3$

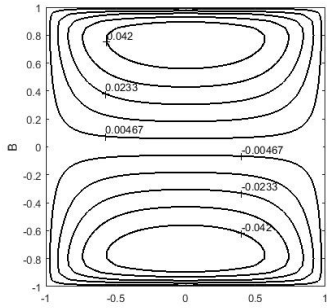

(h) $\alpha = 0.3$

Figure 3.9: Case 3: Velocity and induced magnetic field for $Ha = 10$, $c = 0$.

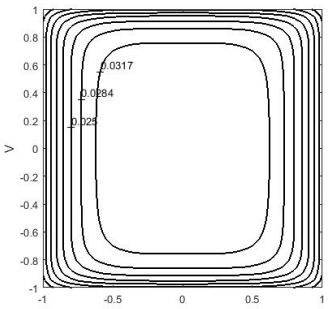

(a) $Ha = 10, N = 40$

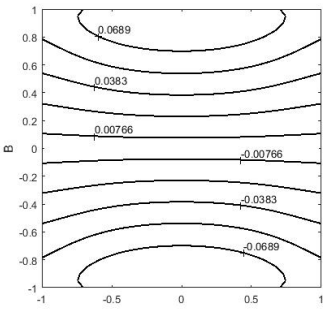

(b) $Ha = 10, N = 40$

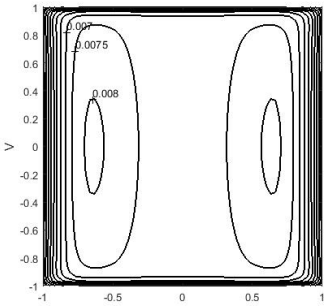

(c) $Ha = 30, N = 60$

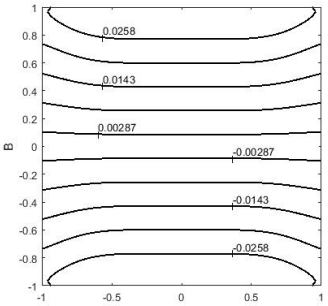

(d) $Ha = 30, N = 60$

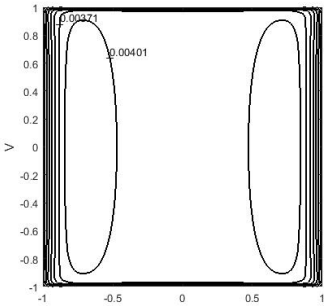

(e) $Ha = 50, N = 80$

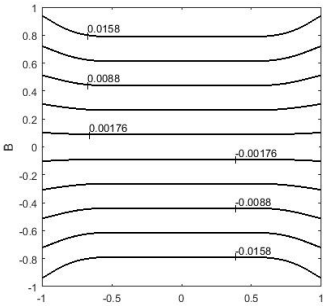

(f) $Ha = 50, N = 80$

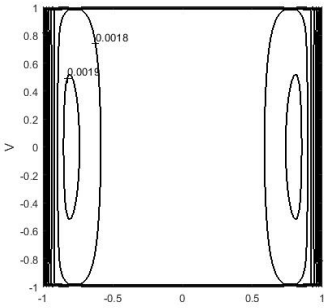

(g) $Ha = 100, N = 100$

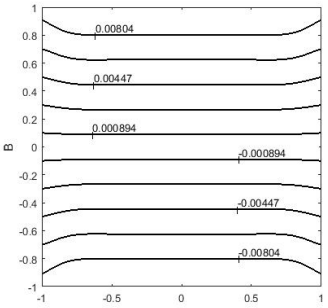

(h) $Ha = 100, N = 100$

Figure 3.10: Case 4: Velocity and induced magnetic field for $\alpha = 0.1$, $c = 2$.

- **Case 5.** Insulated side walls (c=0) , perfectly conducting Hartmann walls ($c \to \infty$), $\alpha = 0$.

Figure 3.11 shows the velocity and induced magnetic field profiles for increasing values of Ha when the Hartmann walls are perfectly conducting but side walls are insulated. As in the Case 1, an increase in Ha caused both the velocity and the induced magnetic field magnitudes to decrease. For large values of Hartmann number Ha, the velocity in the core is relatively low and it gradually increases when it approaches to the side walls.

On the other hand, we have a reverse situation for small values of Hartmann number Ha in which maximum velocity occurs through the center of the duct. Since we have well conducting Hartmann walls, the induced magnetic field becomes perpendicular to these walls for small values of Ha. However, this behavior is overwhelmed with the formation of side walls when Ha increases. The increase in Ha causes the formation of side layers for both the velocity and the induced magnetic field.

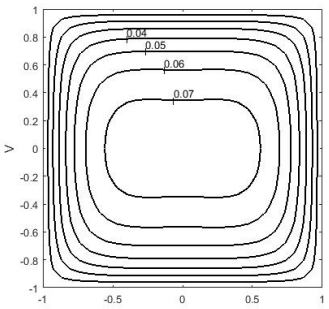

(a) $Ha = 5$, $N = 30$

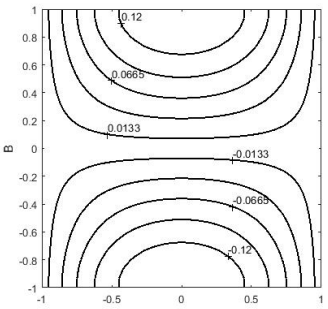

(b) $Ha = 5$, $N = 30$

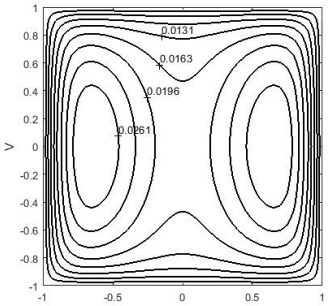

(c) $Ha = 10$, $N = 40$

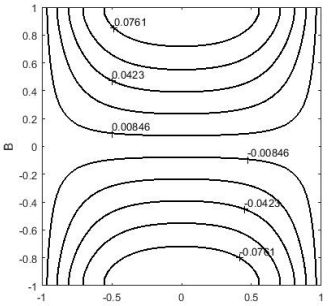

(d) $Ha = 10$, $N = 40$

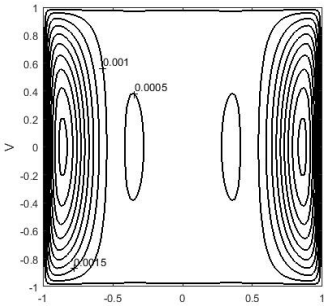

(e) $Ha = 50$, $N = 80$

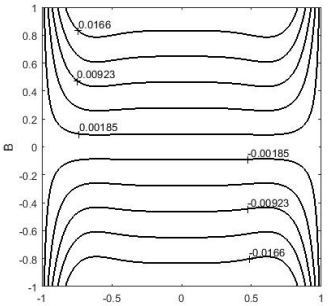

(f) $Ha = 50$, $N = 80$

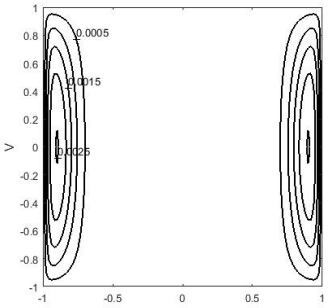

(g) $Ha = 100$, $N = 100$

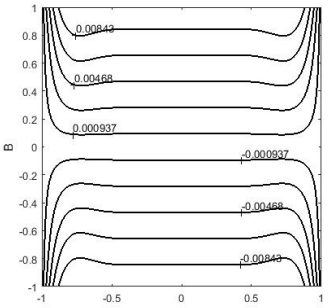

(h) $Ha = 100$, $N = 100$

Figure 3.11: Case 5: Equal velocity and current lines, $\alpha = 0$

In this chapter, the finite difference method (FDM) is used to solve the problem of 2D MHD channel flow in a square duct with different type of boundary conditions. Thus, the numerical results make us to understand the effects of the Hartmann number Ha, the conductivity parameter c and the slipping length α on both of the velocity and the induced magnetic field. As a common character of both the velocity and the induced magnetic field, it is observed that as Ha increases, their magnitudes decrease. Also, the velocity magnitude increases with an increasing value of slipping length α but this increase decelerates when Hartmann number Ha increases. Furthermore, the slip diminishes with an increasing values of Ha. The conductivity parameter c presents the profiles of induced magnetic field from insulated to perfectly conducting plates. The number of discretized points taken on each side of the duct needs to be increased as Ha increases.

CHAPTER 4

CONCLUSION

In this thesis, the application of the finite difference method to the problems of Hartmann flow between parallel plates and the MHD channel flow have been investigated. The one-dimensional and also the two-dimensional, steady, fully-developed and laminar flows of an electrically conducting fluid are solved between parallel plates and in a rectangular duct, respectively, for the fluid velocity and the induced magnetic field. Mixed type boundary conditions are considered for both the velocity and the induced magnetic field which contain no-slip to slipping velocity and insulated to perfectly conducting induced current wall conditions. The effects of the applied magnetic field, ranges of the slip and conductivity values on the flow and induced current are shown in terms of equivelocity and equal induced magnetic field lines for several values of Ha, slip length α and conductivity constant c.

The FDM solutions of the Hartmann flow (1D MHD flow) are compared with the exact solution obtained in this thesis for the most general velocity and induced magnetic field boundary conditions, and the agreement is very well. On the other hand, for the 2D MHD duct flow, the numerical results are compared with the exact solution for the case of no-slip and insulated duct walls and the very well agreement is again seen. The velocity and the induced magnetic field are simulated for five cases of boundary conditions. The findings for both 1D and 2D MHD flow are as follows.

It has been observed that as Ha increases, both the velocity and the induced magnetic field magnitudes decrease. This is the well-known flattening tendency of MHD flow when the external magnetic field is strong. Thus, as Ha increases,

we need to take more mesh points on the sides of the duct since the MHD equations become convection dominated. Besides, it has been noticed that as Ha increases boundary layers are formed near the walls (Hartmann layers on the perpendicular walls and side layers on parallel walls to the external magnetic field). The influence of the slipping length and the conductivity constant on the solution are analyzed by increasing values of these parameters. The increase in the slip length causes an increase in the velocity magnitude, too, which is weakened for large values of Hartmann number. The slip of the velocity on the walls tends to diminish when Ha rises. When the slipping length is kept fixed, the induced magnetic field magnitude increases with an increase in the conductivity parameter whereas the velocity magnitude drops. Conductivity parameter c gives induced magnetic field profiles between the insulated and the perfectly conducting walls. Consequently, we see that the well-known characteristics of the MHD flow are caught and the effects of slip and variable conductivity of the walls are very well depicted with the numerical results obtained easily from the FDM at a cheap expense.

REFERENCES

[1] C. Bozkaya and M. Tezer-Sezgin. Fundamental solution for coupled magnetohydrodynamic flow equations. *Journal of computational and applied mathematics*, 203(1):125–144, 2007.

[2] A. Carabineanu, A. Dinu, and I. Oprea. The application of the boundary element method to the magnetohydrodynamic duct flow. *Zeitschrift für angewandte Mathematik und Physik ZAMP*, 46(6):971–981, 1995.

[3] M. Chutia and P. Deka. Numerical solution for coupled mhd flow equations in a square duct in the presence of strong inclined magnetic field. *International Journal of Advanced Research in Physical Science (IJARPS)*, 2(9):20–29, 2015.

[4] L. Dragos. Magnetofluid dynamics. *Translation of Magnetodinamica fluidelor, Bucharest, Editura Academiei Romane, 1969. Bucharest, Editura Academiei; Tunbridge Wells, Kent, England, Abacus Press, 1975. 478 p.*, 1975.

[5] R. Gold. Magnetohydrodynamic pipe flow. part 1. *Journal of Fluid Mechanics*, 13(4):505–512, 1962.

[6] J. Hartmann and F. Lazarus. *Hg-dynamics*. Levin & Munksgaard Copenhagen, 1937.

[7] H. Hosseinzadeh, M. Dehghan, and D. Mirzaei. The boundary elements method for magneto-hydrodynamic (mhd) channel flows at high hartmann numbers. *Applied Mathematical Modelling*, 37(4):2337–2351, 2013.

[8] J. Hunt and K. Stewartson. Magnetohydrodynamic flow in rectangular ducts. ii. *Journal of fluid mechanics*, 23(3):563–581, 1965.

[9] H.-W. Liu and S.-P. Zhu. The dual reciprocity boundary element method for magnetohydrodynamic channel flows. *The ANZIAM Journal*, 44(2):305–322, 2002.

[10] U. Müller and L. Bühler. *Magnetofluiddynamics in Channels and Containers*. Springer, New York, 2001.

[11] M. Rivero and S. Cuevas. Analysis of the slip condition in magnetohydrodynamic (mhd) micropumps. *Sensors and actuators B: Chemical*, 166:884–892, 2012.

[12] J. Shercliff. Steady motion of conducting fluids in pipes under transverse magnetic fields. In *Mathematical Proceedings of the Cambridge Philosophical Society*, volume 49, pages 136–144. Cambridge University Press, 1953.

[13] B. Singh and J. Lal. Mhd axial flow in a triangular pipe under transverse magnetic field parallel to a side of the triangle. 17, 05 1979.

[14] B. Singh and J. Lal. Finite element method in magnetohydrodynamic channel flow problems. *International Journal for Numerical Methods in Engineering*, 18(7):1104–1111, 1982.

[15] S. Smolentsev. Mhd duct flows under hydrodynamic "slip" condition. *Theoretical and Computational Fluid Dynamics*, 23(6):557, 2009.

[16] Z. Tao and M. Ni. Analytical solutions for mhd flow at a rectangular duct with unsymmetrical walls of arbitrary conductivity. *Science China Physics, Mechanics & Astronomy*, 58(2):1–18, 2015.

[17] D. J. Temperley and L. Todd. The effects of wall conductivity in magnetohydrodynamic duct flow at high hartmann numbers. *Mathematical Proceedings of the Cambridge Philosophical Society*, 69(2):337–351, 1971.

[18] M. Tezer-Sezgin. Boundary element method solution of mhd flow in a rectangular duct. *International journal for numerical methods in fluids*, 18(10):937–952, 1994.

[19] M. Tezer-Sezgin and C. Bozkaya. Boundary element method solution of magnetohydrodynamic flow in a rectangular duct with conducting walls parallel to applied magnetic field. *Computational Mechanics*, 41(6):769–775, 2008.

[20] M. Tezer-Sezgin and S. Köksal. Finite element method for solving mhd flow in a rectangular duct. *International journal for numerical methods in engineering*, 28(2):445–459, 1989.